INFECTION AND IMMUNITY, Nov. 2011, p. 4523–4532 Vol. 79, No. 11
0019-9567/11/$12.00 doi:10.1128/IAI.05412-11

Discovery of GAMA, a *Plasmodium falciparum* Merozoite Micronemal Protein, as a Novel Blood-Stage Vaccine Candidate Antigen▽‡

Thangavelu U. Arumugam,[1] Satoru Takeo,[1] Tsutomu Yamasaki,[1] Amporn Thonkukiatkul,[3] Kazutoyo Miura,[4] Hitoshi Otsuki,[5] Hong Zhou,[4] Carole A. Long,[4] Jetsumon Sattabongkot,[6]† Jennifer Thompson,[7] Danny W. Wilson,[7] James G. Beeson,[8] Julie Healer,[7] Brendan S. Crabb,[8] Alan F. Cowman,[7] Motomi Torii,[9,10] and Takafumi Tsuboi[1,2,10]*

Cell-Free Science and Technology Research Center[1] and Venture Business Laboratory,[2] Ehime University, Matsuyama, Ehime 790-8577, Japan; Department of Biology, Faculty of Science, Burapha University, Chonburi 20131, Thailand[3]; Laboratory of Malaria and Vector Research, National Institute of Allergy and Infectious Diseases, National Institutes of Health, Rockville, Maryland[4]; Division of Medical Zoology, Faculty of Medicine, Tottori University, Yonago, Tottori 683-8503, Japan[5]; Entomology Department, Armed Forces Research Institute of Medical Sciences, Bangkok 10400, Thailand[6]; The Walter and Eliza Hall Institute for Medical Research, Melbourne, Victoria 3052, Australia[7]; Burnet Institute, Melbourne, Victoria 3004, Australia[8]; Department of Molecular Parasitology, Ehime University Graduate School of Medicine, Toon, Ehime 791-0295, Japan[9]; and Ehime Proteo-Medicine Research Center, Ehime University, Toon, Ehime 791-0295, Japan[10]

Received 19 May 2011/Returned for modification 20 June 2011/Accepted 24 August 2011

One of the solutions for reducing the global mortality and morbidity due to malaria is multivalent vaccines comprising antigens of several life cycle stages of the malarial parasite. Hence, there is a need for supplementing the current set of malaria vaccine candidate antigens. Here, we aimed to characterize glycosylphosphatidylinositol (GPI)-anchored micronemal antigen (GAMA) encoded by the PF08_0008 gene in *Plasmodium falciparum*. Antibodies were raised against recombinant GAMA synthesized by using a wheat germ cell-free system. Immunoelectron microscopy demonstrated for the first time that GAMA is a microneme protein of the merozoite. Erythrocyte binding assays revealed that GAMA possesses an erythrocyte binding epitope in the C-terminal region and it binds a nonsialylated protein receptor on human erythrocytes. Growth inhibition assays revealed that anti-GAMA antibodies can inhibit *P. falciparum* invasion in a dose-dependent manner and GAMA plays a role in the sialic acid (SA)-independent invasion pathway. Anti-GAMA antibodies in combination with anti-erythrocyte binding antigen 175 exhibited a significantly higher level of invasion inhibition, supporting the rationale that targeting of both SA-dependent and SA-independent ligands/pathways is better than targeting either of them alone. Human sera collected from areas of malaria endemicity in Mali and Thailand recognized GAMA. Since GAMA in *P. falciparum* is refractory to gene knockout attempts, it is essential to parasite invasion. Overall, our study indicates that GAMA is a novel blood-stage vaccine candidate antigen.

Plasmodium falciparum is the causative agent of the most burdensome form of human malaria, affecting about 225 million individuals and killing about 0.8 million individuals in 2009 worldwide (37). The reemergence of drug-resistant parasites and insecticide-resistant mosquitoes aggravates the spread of malaria (19). The complex biology, extensive antigenic diversity, and immune evasion strategies of *P. falciparum* enable it to cause repeated and chronic infections. However, naturally acquired immunity to malaria does develop after repeated exposure (27), and several lines of evidence support the feasibility of vaccines to protect against malaria (16). The scope and expectation for malaria vaccine development have expanded dramatically in recent years, in large part due to the renewed focus on control, local elimination, and eventual global eradication efforts (3). However, despite intensive efforts, no malaria vaccine has yet been licensed, and there is an urgency to rapidly enrich the pipeline of vaccine development with novel vaccine candidates. The availability of the *P. falciparum* genome sequence, along with its transcription and proteomic profiles and insights, has provided great opportunities to identify new candidates for development into vaccines (15).

Highly efficacious malaria vaccines will certainly need to be multicomponent vaccines that comprise several different alleles of an antigen and/or several different antigens and/or comprise antigens of several life cycle stages to overcome the antigenic diversity and immune evasion capacity of *P. falciparum* and, hence, provide broad and sustained protection. This provides a strong rationale for developing blood-stage vaccines as part of the strategy (27). Although an increasing number of merozoite antigens are being identified, few antigens have been evaluated as vaccine candidates or as targets of immunity (14, 27). Therefore, we were interested in identifying novel blood-stage vaccine candidate antigens.

* Corresponding author. Mailing address: Cell-Free Science and Technology Research Center, Ehime University, 3 Bunkyo-cho, Matsuyama, Ehime 790-8577, Japan. Phone: 81-89-927-8277. Fax: 81-89-927-9941. E-mail: tsuboi@ccr.ehime-u.ac.jp.

† Present address: Mahidol Vivax Research Center, Faculty of Tropical Medicine, Mahidol University, Bangkok, Thailand.

‡ Supplemental material for this article may be found at http://iai.asm.org/.

▽ Published ahead of print on 6 September 2011.

In order to find novel blood-stage vaccine candidates, basic research on the molecular basis of invasion and subsequent modification of the host cell is indispensable. The invasion-related merozoite proteins are either located on the merozoite surface (mostly via glycosylphosphatidylinositol [GPI] anchors) or stored initially in apical organelles (i.e., micronemes, rhoptries, and dense granules) and later translocated onto the surface of the invading parasite. Since these proteins are eventually exposed to the human immune system, they are leading blood-stage vaccine candidate antigens (18, 20). For instance, merozoite surface proteins 1 and 2 (MSP1 and MSP2, respectively) and the micronemal protein apical membrane antigen 1 (AMA1) have been explored as blood-stage vaccine candidates (27) and as targets of acquired human immunity (14).

Therefore, this study was taken up with the objective of identifying previously uncharacterized *P. falciparum* proteins that are targeted to either apical organelles or the parasite surface and assess them as novel blood-stage vaccine candidates. For this purpose, we used *P. falciparum* genome (15), transcriptome (4), and proteome (13) data as a starting point and screened the proteins in this data set based on four features: (i) late-schizont stage transcription, (ii) smaller gene size (<2.5 kbp), (iii) presence of predicted signal peptide (SP), and (iv) putative GPI anchor attachment site. Our bioinformatics searches identified PF08_0008 as a novel putative surface and/or apical protein. Previous bioinformatics searches by Haase et al. (using transcriptional and structural features) (20) and Gilson et al. (using their GPI anchor site prediction software trained on *P. falciparum* sequences) (18) have also predicted that PF08_0008 may be an invasion-related, surface or apical organellar, merozoite antigen. Recently, Hinds et al. (21) have experimentally shown that PF08_0008 is a novel GPI-anchored erythrocyte binding protein that appears to be localized in the apical organelle of *P. falciparum* merozoites and, hence, designated the protein GPI-anchored micronemal antigen (GAMA). However, antibodies (Abs) raised against recombinant GAMA expressed in *Escherichia coli* were not inhibitory to invasion or growth of the parasite, and therefore, the role of GAMA as a vaccine candidate antigen is unclear (21). In our previous studies (32, 34, 35), we have demonstrated that the wheat germ cell-free system is an optimal system for the synthesis of correctly folded recombinant malaria proteins in sufficient quantities. Therefore, in this study, we attempted to test our hypothesis that GAMA may be a vaccine candidate by using recombinant GAMA expressed in the wheat germ cell-free system and further define its subcellular localization by immunoelectron microscopy (IEM) and characterize its erythrocyte binding region and its receptor on the erythrocyte membrane.

MATERIALS AND METHODS

Parasite culture and culture supernatant. *P. falciparum* asexual stages (3D7 strain) were cultured *in vitro* in human erythrocytes (blood group O+ or A+) obtained from the Japanese Red Cross Society as previously described (6). To harvest parasite pellets, mature schizonts were purified by using Percoll (GE Healthcare, Camarillo, CA) density gradient centrifugation and further treated with tetanolysin, washed with phosphate-buffered saline (PBS) containing Complete protease inhibitor (Roche, Mannheim, Germany), and stored at −80°C until used. For culture supernatant preparation, tightly synchronized, purified schizonts were cultured for 20 h at 37°C in the absence of erythrocytes for rupture and merozoite release. The culture medium was centrifuged at 3,000 × *g* for 20 min at 4°C to remove cellular debris, and subsequently, the supernatant was concentrated 5-fold in a centrifugal filter (Amicon Ultra 10K device; Millipore, Billerica, MA) and stored in aliquots at −80°C until used.

RNA isolation and cDNA synthesis. Total RNA was isolated from 3D7 parasite-infected erythrocytes rich in schizonts by using the RNeasy minikit (Qiagen, Hilden, Germany) and stored at −80°C. Following DNase treatment, cDNA was generated with random hexamers by using an Omniscript reverse transcription kit (Qiagen).

Production of recombinant PF08_0008 proteins and antisera. The nucleotide sequence of the PF08_0008 gene was obtained from the *P. falciparum* 3D7 genome database (http://plasmodb.org). Full-length and different truncated versions of PF08_0008 proteins were synthesized and used for raising antibodies (see Fig. 1). Briefly, the *PF08_0008* fragments encoding constructs designated FL (full-length GAMA, comprising amino acid [aa] 1 to aa 738), ECTO (full-length GAMA without signal peptide and transmembrane [TM] regions and comprising aa 25 to aa 714 and a hexahistidine [His] tag at the C terminus), Tr1 (truncated protein 1; comprising aa 25 to aa 337 and a His tag at the C terminus), and Tr3 (truncated protein 3; comprising aa 500 to aa 714 and a His tag at the C terminus) were amplified by using sense primers with XhoI sites and antisense primers with NotI restriction sites (shown in lowercase letters in the primer sequences below), by PCR from *P. falciparum* 3D7 cDNA. The primer pairs FLf (5′-ctcgagATGAAATATTATACATCTTTGTACGTTGC-3′) and FLr (5′-gcggccgcCTAATTTAACAAGTTAATTAAAATGAACGAAAAAA AAAGG-3′), ECTOf (5′-ctcgagaTGAATTCGAACACTCCTCAGGCCTTC-3′) and ECTOr (5′-gcggccgcCTAATGATGATGATGATGGTGTGCCTTTG CATTTGGTCCTTGAAAAG-3′), Tr1f (5′-ctcgagATGAATTCGAACACTC CTCAGGCCTTC-3′) and Tr1r (5′-gcggccgcCTAATGATGATGATGATGG TGATGCTTATATGCATTTAGTTTATTAAGTATATC-3′), and Tr3f (5′-c tcgagATGAAGGATATTATAAAATTATTAAAAGATTTAATAAAATAT TTAC-3′) and Tr3r (5′-gcggccgcCTAATGATGATGATGATGGTGTGCCT TTGCATTTGGTCCTTGAAAAG-3′) were used to generate the DNA fragments encoding FL, ECTO, Tr1, and Tr3 proteins, respectively. The underlined sequences in the primers above indicate the regions that encode His tags.

The amplified fragments were then restricted and ligated into the wheat germ cell-free expression vectors (CellFree Sciences, Matsuyama, Japan). Fragments of ECTO, Tr1, and Tr3 were cloned into the pEU-E01-MCS vector. Fragments of FL were cloned into the pEU-E01-GST-TEV-N2 vector. The cloned inserts were sequenced by using an ABI PRISM 3100-Avant genetic analyzer (Applied Biosystems, Foster City, CA). The recombinant proteins with either glutathione *S*-transferase (GST) or His tags were expressed using a wheat germ cell-free system (CellFree Sciences) and purified using either a glutathione-Sepharose 4B column (GE Healthcare) or a nickel-Sepharose column (GE Healthcare) as described previously (36). Only in the case of the full-length protein, the N-terminal GST tag was removed by eluting GST-tagged FL bound to a glutathione-Sepharose 4B column by using tobacco etch virus (TEV) protease which cleaves the TEV recognition site between the GST tag and full-length GAMA. To generate antisera of these proteins (FL without GST tag, ECTO, Tr1, and Tr3), two BALB/c mice were immunized subcutaneously with 20 μg of purified recombinant proteins emulsified with Freund's complete adjuvant, followed by 20 μg of the proteins with Freund's incomplete adjuvant thereafter. Japanese white rabbits were immunized subcutaneously with 250 μg of purified proteins with Freund's complete adjuvant, followed by 250 μg of purified proteins with Freund's incomplete adjuvant thereafter. All immunizations were done 3 times at 3-week intervals. The antisera were collected 14 days after the last immunization. All animal experimental protocols were approved by the Institutional Animal Care and Use Committee of Ehime University, and the experiments were conducted according to the Ethical Guidelines for Animal Experiments of Ehime University. The rabbit anti-erythrocyte binding antigen 175 (regions 3 to 5) (EBA175) serum was prepared as previously described (22).

Western blot analysis. For the analysis of total schizont material, purified parasite pellets were directly lysed in an appropriate amount of 2× reducing or nonreducing SDS-PAGE sample buffer. The lysate was centrifuged at 10,000 × *g* for 10 min at room temperature (RT), and supernatants were collected, boiled at 95°C for 10 min, and resolved by electrophoresis in a 12.5% polyacrylamide gel (ATTO, Tokyo, Japan). Proteins were then transferred onto a 0.2-μm polyvinylidene difluoride (PVDF) membrane (Hybond LFP; GE Healthcare). The membranes were blocked with PBSTM buffer (PBS containing 0.1% [vol/vol] Tween 20 and 5% [wt/vol] nonfat milk) and then probed with appropriate primary antibodies diluted in PBSTM buffer. Bound primary antibodies were detected by incubation with an appropriate horseradish peroxidase (HRP)-conjugated secondary antibody (GE Healthcare) diluted in PBSTM buffer, followed by visualization reaction with Immobilon Western chemiluminescent HRP sub-

strate (Millipore). The relative molecular sizes of the proteins were calculated with reference to a molecular weight size marker (MagicMark XP; Invitrogen, Carlsbad, CA).

Indirect immunofluorescence assay (IFA). *P. falciparum* (3D7) blood-stage parasites were cultured to approximately 8% parasitemia as previously described (6). Blood smears were prepared on glass slides when the majority of the parasites were at late trophozoite and schizont stages. Then, slides were fixed with ice-cold acetone for 3 min, dried, and stored at −80°C. Before use, the slides were thawed and blocked with PBS containing 5% nonfat milk at 37°C for 30 min. After the blocking, the slides were incubated with primary antibodies (both rabbit anti-FL and mouse anti-*P. falciparum* apical membrane antigen 1 [PfAMA1]) at 37°C for 1 h, followed by Alexa 488-conjugated goat anti-rabbit IgG secondary Ab (Invitrogen), Alexa 546-conjugated goat anti-mouse IgG secondary Ab (Invitrogen), and nuclear stain with DAPI (4′,6-diamidino-2-phenylindole) at 37°C for 30 min. The slides were mounted in ProLong Gold antifade reagent (Invitrogen) and visualized under oil immersion in a confocal scanning laser microscope (LSM5 PASCAL; Carl Zeiss MicroImaging, Thornwood, NY) using a Plan-Apochromat 63×/1.4 oil differential interference contrast (DIC) objective lens. Images were captured with LSM5 PASCAL software and prepared for publication with Adobe Photoshop (Adobe Systems, San Jose, CA).

IEM. The purification of Tr3-specific IgGs from protein G-purified total rabbit IgGs raised against Tr3 was done using an antigen affinity chromatography method. One milligram of purified recombinant Tr3 was buffer exchanged into coupling buffer (0.2 M $NaHCO_3$, 0.5 M NaCl) by using PD-10 desalting columns (GE Healthcare) and covalently coupled to a HiTrap *N*-hydroxysuccinimide (NHS)-activated HP column (GE Healthcare) according to the manufacturer's protocol. By use of this antigen column, Tr3-specific IgG was purified from total rabbit IgG raised against Tr3 protein. For immunoelectron microscopy (IEM), schizont stages of parasites were fixed for 15 min on ice in a mixture of 1% paraformaldehyde–0.1% glutaraldehyde in 0.1 M phosphate buffer (pH 7.4). Fixed specimens were washed, dehydrated, and embedded in LR White resin (Polysciences, Warrington, PA) as previously described (6). Ultrathin sections were blocked at 37°C for 30 min in PBS containing 5% nonfat milk and 0.01% Tween 20 (PBS-MT). The grids were then incubated at 4°C overnight with rabbit Tr3-specific IgG or control sera in PBS-MT. After washing with PBS containing 10% Block Ace (Yukijirushi, Sapporo, Japan) and 0.01% Tween 20 (PBS-BT), the grids were incubated at 37°C for 1 h with goat anti-rabbit IgG conjugated to 10-nm gold particles (Amersham Life Science, Arlington, IL) diluted 1:20 in PBS-MT, rinsed with PBS-BT, and fixed on ice for 10 min in 2.5% glutaraldehyde to stabilize the gold. The grids were then rinsed with distilled water, dried, and stained with uranyl acetate and lead citrate. Samples were examined with a transmission electron microscope (JEM-1230; JEOL, Tokyo, Japan).

Erythrocyte binding assay. Pure human erythrocytes were obtained from the Japanese Red Cross Society. It was stored at 4°C for up to 4 weeks and washed three times in incomplete RPMI medium (iRPMI; RPMI 1640 medium with L-glutamine, 25 mM HEPES buffer, and 50 mg/liter of hypoxanthine without sodium bicarbonate [Invitrogen]) before use. Enzyme treatments of erythrocytes were done as previously described (9). Briefly, sialic acid (SA) residues were removed by incubating 100 μl of packed human erythrocytes with neuraminidase (final concentration [fc] of 66.7 mU/ml in iRPMI), on a rotating wheel, for 1 h at 37°C. For trypsin or chymotrypsin treatment, 100 μl of packed human erythrocytes was incubated with trypsin or chymotrypsin (final concentration of 1 mg/ml in iRPMI), on a rotating wheel, for 1 h at 37°C and subsequently incubated with soybean trypsin inhibitor (final concentration of 0.5 mg/ml in iRPMI) for 10 min at 37°C to inhibit the trypsin or chymotrypsin. After the enzyme treatments, the erythrocytes were washed twice with 10 ml of iRPMI, then resuspended in iRPMI at a 50% hematocrit, stored at 4°C, and used within a week.

For erythrocyte binding assays with recombinant GAMA, 5 to 10 μg of recombinant protein (either ECTO, Tr1, or Tr3) was incubated with 100 μl of untreated, neuraminidase-treated, trypsin-treated, or chymotrypsin-treated human erythrocytes on a rotating wheel for 30 min at RT. After the incubation, the reaction mixture was layered over silicone oil (HIVAC F4; Shin-Etsu Silicones, Tokyo, Japan) and centrifuged in order to remove unbound proteins in the supernatant and collect pelleted erythrocytes. Proteins bound to erythrocytes were either eluted directly from the pelleted erythrocytes or eluted after the pelleted erythrocytes were washed once with iRPMI. Elution was done by incubating erythrocytes with 20 μl of 0.5 M NaCl in PBS, pH 7.4, for 15 min at RT. An amount of 2× SDS reducing sample buffer equal to the 20μl NaCl in PBS was added to the eluted proteins and incubated at 37°C for 20 min. The samples were separated by SDS-PAGE and detected by Western blotting using mouse monoclonal anti-penta-His antibodies (Qiagen).

For the erythrocyte binding assay with native GAMA and EBA175 shed in the culture supernatant, 100 μl of five-times-concentrated culture supernatant was incubated with 100 μl of untreated and enzyme-treated human erythrocytes, on a rotating wheel, for 30 min at RT. The reaction mixture was then layered over silicone oil and centrifuged to collect erythrocytes. Bound protein was eluted from the pelleted erythrocytes by incubating erythrocytes with 20 μl of 0.5 M NaCl in PBS, pH 7.4, for 15 min at RT. An amount of 2× SDS nonreducing sample buffer equal to the 20μl NaCl in PBS was added to the eluted proteins and incubated at 37°C for 20 min. The samples were separated by SDS-PAGE and detected by Western blotting using the respective rabbit antibodies.

To check whether Tr3 binds to the receptor of native GAMA (see Fig. 5B), the following seven erythrocyte binding reactions were done using the procedure described above: (i) erythrocytes were incubated with 10 μg of Tr3, (ii) erythrocytes were incubated initially with 10 μg of GST followed by centrifugation, removal of supernatant containing the unbound GST fraction, and subsequent incubation with 10 μg of Tr3, (iii) erythrocytes were incubated initially with 10 μg of Tr1 followed by centrifugation, removal of supernatant containing the unbound Tr1 fraction, and subsequent incubation with 10 μg of Tr3, (iv) erythrocytes were incubated with a mixture containing 10 μg each of Tr1 and Tr3, (v) erythrocytes were incubated initially with 100 μl of 5-times-concentrated culture supernatant followed by centrifugation, removal of supernatant, and subsequent incubation with 10 μg of Tr3, (vi) erythrocytes were incubated with 100 μl of 5-times-concentrated culture supernatant, and (vii) erythrocytes were incubated initially with 10 μg of Tr3, followed by centrifugation, removal of supernatant containing the unbound Tr3 fraction, and subsequent incubation with 100 μl of 5-times-concentrated culture supernatant. After the final incubations, bound proteins were eluted as described above, and the quantities of Tr3 and native GAMA proteins in eluted proteins were detected by Western blotting with anti-penta-His and anti-FL antibodies, respectively.

GIA. Total IgGs to be tested in a growth inhibition assay (GIA) were purified from rabbit antisera with HiTrap protein G Sepharose columns (GE Healthcare) according to the manufacturer's protocol. Purified antibodies were further buffer exchanged into iRPMI, concentrated using Amicon Ultra-15 centrifugal devices (Millipore), filter sterilized using Ultrafree-MC GV 0.22-μm tubes (Millipore), and preabsorbed using 25 μl of packed human O+ erythrocytes per purified IgG from 1 ml of antiserum for 1 h at RT on a shaker. Finally, the concentrations of all antibodies were adjusted to 40 mg/ml in iRPMI. The inhibitory activity of antibodies was tested over one cycle of parasite replication, and parasitemia was measured by flow cytometry as described previously (2, 25). Briefly, the parasite cultures were synchronized the day before the start of the GIA. At the commencement of the GIA, the majority of parasites were at the late trophozoite to schizont stage. Twenty microliters of parasite suspension (0.3% parasitemia and 2% hematocrit) and 20 μl of antibodies were added per well of half-area flat-bottom 96-well cell culture microplates (Corning, Corning, NY) and gently mixed. For a control, 20 μl of iRPMI was added to the parasite suspension. Cultures were incubated at 37°C in a humidified, gassed (90% N_2, 5% O_2, and 5% CO_2) box. After 25 h of incubation, the cultures were pelleted via centrifugation (1,300 × *g* for 5 min) and washed in 100 μl PBS. The cells were then incubated with 50 μl of diluted (1:1,000 in PBS) SYBR green I nucleic acid gel stain (Invitrogen) for 10 min at RT. Cells were washed once in PBS and resuspended in PBS. Parasitemia was measured by flow cytometry using a FACSCantII (BD Biosciences, San Jose, CA) with an acquisition of 50,000 events per sample. Data were analyzed with FlowJo 9.1 software (Tree Star, Ashley, OR). Samples were tested in triplicate in each experiment, and three independent experiments were performed. The GIA based on the parasite lactate dehydrogenase (pLDH) assay was done as previously described (8). Antibodies were also tested for inhibitory activity over two cycles of parasite replication, as described previously, with parasitemia measured by flow cytometry (24, 25); antibodies were tested at a 1/10 dilution (final concentration of 2 or 4 mg/ml). In these assays, inhibition of growth by antibodies greater than 10% compared to the control values is considered significant (25, 38). For GIAs using neuraminidase-treated erythrocytes, erythrocytes were treated with neuraminidase (final concentration of 66.7 mU/ml in iRPMI), on a rotating wheel, for 1 h at 37°C and washed twice with 10 ml of iRPMI, then resuspended in iRPMI at a 50% hematocrit, stored at 4°C, and used within a week.

ELISA. Human plasma samples were collected from adults living in three areas of malaria endemicity in Mali (29). The study was approved by the ethical review committees of the Faculty of Medicine, Pharmacy, and Dentistry at the University of Bamako (Mali) and the NIAID, National Institutes of Health (Bethesda, MD). Individual written informed consent was obtained from all participants. Human serum samples from Thailand were collected from asymptomatic parasite carriers infected with *P. falciparum* alone with written informed consent as previously described (7). The study was approved by the Ethics

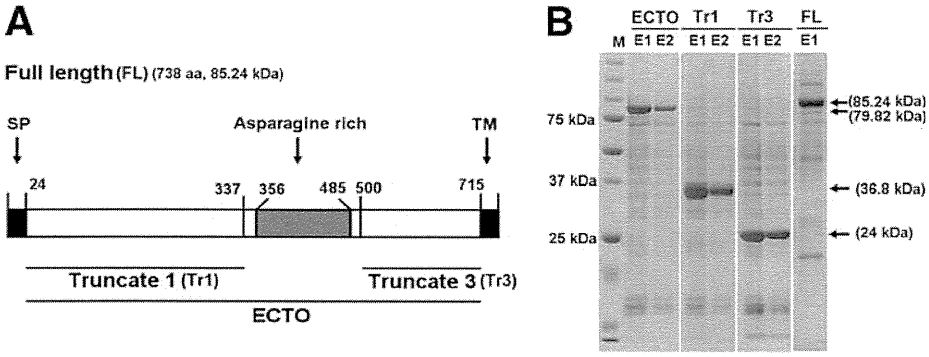

FIG. 1. Structure and recombinant proteins of GAMA. (A) Schematic of the primary structure of GAMA. The GAMA protein consists of 738 amino acids, with a calculated molecular mass of 85.24 kDa. Indicated are the predicted signal peptide (SP; residues 1 to 24), asparagine-rich region (residues 356 to 485), and C-terminal transmembrane domain (TM; residues 715 to 738). FL GAMA (residues 1 to 738) and three regions of GAMA (Tr1 [residues 25 to 337], Tr3 [residues 500 to 714], and ECTO [residues 25 to 714]) were expressed in recombinant form and used to raise specific antisera. (B) SDS-PAGE of recombinant proteins of GAMA. All the recombinant proteins were synthesized using a wheat germ cell-free protein expression system. The fractions of purified ECTO (79.82 kDa), Tr1 (36.8 kDa), Tr3 (24 kDa), and FL (85.24 kDa) proteins resolved in an SDS-PAGE gel and stained with Coomassie brilliant blue R-250 are shown. M represents a molecular weight marker. E1 and E2 represent the first and the second fractions of purified proteins eluted from affinity purification columns, respectively. Arrows indicate specific bands.

Committee of the Thai Ministry of Public Health and the Institutional Review Board of the Walter Reed Army Institute of Research (7). Measurement of antibodies against *P. falciparum* GAMA in the 1:1,000-diluted Mali or Thai sera was performed as previously described (29). Briefly, 96-well enzyme-linked immunosorbent assay (ELISA) plates were coated with 50 ng/well of purified FL in coating buffer (20 mM boric acid, pH 8.9) and incubated at 4°C overnight. The plates were blocked with 2 mg/ml of gelatin in coating buffer. The sera were diluted (1:1,000) in phosphate-buffered saline with 0.1% Tween 20 (PBS-T), added to antigen-coated wells in duplicate, and incubated for 1 h at 37°C. After the plates were washed, they were incubated with 1:3,000-diluted HRP-conjugated rabbit anti-human IgG (DakoCytomation, Glostrup, Denmark) in PBS-T for 1 h at 37°C. After the plates were washed, they were incubated with 0.5 mg/ml azino-bis-3-ethylbenthiazoline-6-sulfonic acid (Wako, Osaka, Japan) diluted in citrate buffer (0.1 M citric acid, pH 4.1) for 20 min at RT. The reaction was stopped with 0.1 M citric acid, and optical densities (ODs) were measured at 415 nm by using a precision microplate reader (Molecular Devices, Sunnyvale, CA). The ELISA experiments were replicated twice independently.

Statistical analysis. For the ELISA, the Mann-Whitney *U* test was performed. For the GIA, a one-way analysis of variance (ANOVA) was performed. If the overall test was significant, Bonferroni's pairwise multiple-comparison tests were used to compare each experimental group to the control. All statistical analyses were performed using GraphPad Prism (GraphPad Software, San Diego, CA).

RESULTS

Recombinant GAMA proteins and antibodies. Sequence information of GAMA encoded by *PF08_0008* retrieved from PlasmoDB (http://www.plasmodb.org) revealed that GAMA in *P. falciparum* is a 738-amino-acid protein (with a predicted molecular mass of 85.2 kDa) (Fig. 1A). GAMA has a signal peptide (residues 1 to 24), a long asparagine-rich region (residues 356 to 485), and a transmembrane domain (residues 715 to 738) (Fig. 1A). We used the wheat germ cell-free system to synthesize the recombinant full-length GAMA (FL) and truncated versions of GAMA proteins, namely, ECTO (GAMA without the SP and TM regions), Tr1 (region upstream of the asparagine-rich region), and Tr3 (region downstream of the asparagine-rich region), without codon optimization (Fig. 1A and B). Figure 1B shows the different truncated GAMA proteins resolved in a 12.5% SDS-polyacrylamide gel. Almost all of the GAMA proteins were recovered in the supernatant fraction and easily purified as a single dominant band (Fig. 1B, arrows) by affinity chromatography. These results demonstrate that the wheat germ cell-free system is able to translate the native GAMA gene sequences and produce soluble proteins. These proteins were used to immunize rabbits and mice to produce antibodies.

Proteolytic processing and shedding of GAMA into culture supernatant. The Western blotting of schizont material and culture supernatant with anti-GAMA antisera reconfirmed the previous findings (21) that primary (FL to p37-p49 dimer) and secondary (p49 to p42 and residual stub) processing events occur in GAMA (Fig. 2A), and GAMA is shed into culture supernatant as a dimer (p37-p42) following erythrocyte invasion (Fig. 2B). Moreover, p37-p42 and the residual stub were clearly detected in our blot of parasite lysates. These results also confirm the quality and specificity of the different antibodies raised against GAMA synthesized in a wheat germ cell-free system.

Subcellular location of GAMA. To confirm the localization of GAMA, an IFA was performed (Fig. 3A). When the acetone-fixed smears of parasites in the late schizont stage were stained with rabbit anti-FL antiserum, green fluorescence was seen in the apical region (Fig. 3A, top panel), suggesting that GAMA resides in an apical organelle. The colocalization of GAMA with AMA1 indicates that GAMA may be localized in micronemes (Fig. 3A, top panel). These results in Fig. 3A were in good agreement with the previous findings (21). In order to validate the IFA data by electron microscopy, parasites in late schizont stages were stained with Tr3-specific IgGs and subsequently with secondary antibody labeled with gold particles. The signals of gold particles were found in micronemes (Fig. 3B, arrows), indicating that GAMA is indeed a micronemal protein. When free merozoites were stained with anti-FL antiserum, a circumferential green fluorescence was detected on the parasite surface (Fig. 3A, bottom panel), suggesting that GAMA resides on the surface of free merozoites.

GIA. In order to test whether antibodies to GAMA could block parasite invasion, rabbit polyclonal IgG to FL GAMA was tested initially for inhibition of parasite growth over one

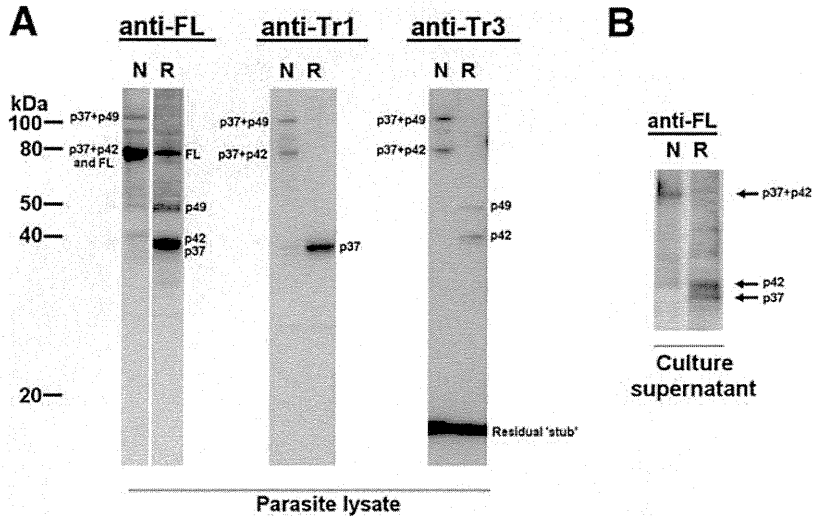

FIG. 2. Processing and shedding of GAMA. (A) Detection of GAMA in schizont lysate. Total schizont material was examined by Western blotting under reducing (R) and nonreducing (N) conditions, using the rabbit anti-FL, mouse anti-Tr1, and rabbit anti-Tr3 antisera. (B) Detection of GAMA in culture supernatant. Culture supernatant was analyzed by Western blotting under reducing and nonreducing conditions using the rabbit anti-FL.

cycle of replication with measurement of parasite growth by using flow cytometry. When anti-FL, anti-AMA1 (positive control), and anti-GST (negative control) were tested at final concentrations of 20 mg/ml (total IgG concentration), they inhibited the invasion by (mean) 38%, 66%, and 9%, respectively (Fig. 4A). Using a GIA based on parasite detection using the pLDH assay, both total and antigen-specific anti-FL IgGs inhibited invasion and/or growth (up to about 43% and 21%, respectively) in a dose-dependent manner (Fig. 4C). IgGs to FL, Tr1, and Tr3 were also tested for their growth-inhibitory activities over two cycles of replication at final concentrations of 2.3 mg/ml, 4 mg/ml, and 4 mg/ml, respectively. The levels of inhibition were (mean ± SEM) 20% ± 2.6%, 32% ± 0.5%, and 20% ± 3.1%, respectively. The normal rabbit IgG at the same concentration gave no significant inhibition (mean ± SEM, 0.3% ± 3.3%).

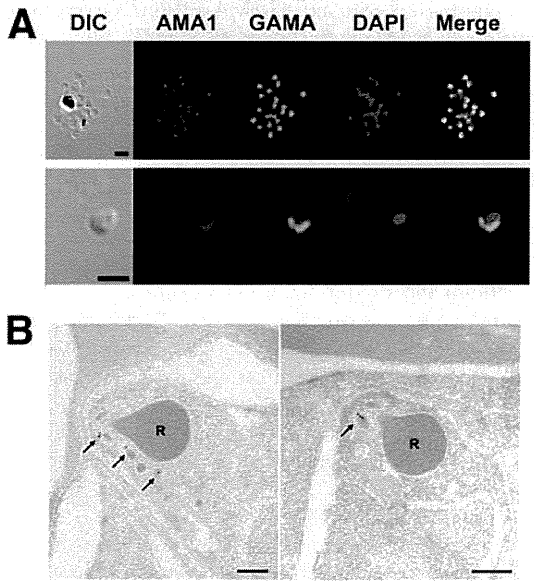

FIG. 3. Localization of GAMA in asexual blood-stage parasites. (A) GAMA localization using an immunofluorescence assay. Acetone-fixed *P. falciparum* 3D7 mature schizonts (top panel) and free merozoites (bottom panel) were probed with rabbit anti-FL (green) and mouse anti-PfAMA1 (microneme marker) (red). Parasite nuclei were stained with DAPI (blue). Scale bars represent 2 μm. (B) GAMA localization using immunoelectron microscopy. The two sections of merozoites in schizont-infected erythrocytes were probed with purified rabbit anti-Tr3 antibody and subsequently by secondary antibody conjugated with gold particles. The arrows indicate the micronemal localization of signals from gold particles. Bars represent 200 nm. Arrows mark micronemes. R's mark rhoptries.

The erythrocyte binding region of GAMA. Hinds et al. have previously reported that native GAMA (p37-p42 heterodimer) in the culture supernatant can bind to erythrocyte membranes and the bound GAMA can be eluted (using 0.5 M NaCl in PBS, pH 7.4) from erythrocyte membranes after extensive washing with PBS (21). However, the location of the erythrocyte binding region of GAMA has not yet been defined. Characterization of the erythrocyte binding region will be helpful for understanding the molecular basis of invasion inhibition by anti-GAMA antibodies that we have observed in our GIA. Therefore, we tested the erythrocyte binding abilities of recombinant GAMA ECTO, Tr1, and Tr3 proteins.

First, we reconfirmed that native GAMA (the p37-p42 dimer), shed by extracellular merozoites into the culture supernatant, has the ability to bind erythrocytes (Fig. 5A), as previously reported (21). Second, we tested the erythrocyte binding abilities of the recombinant proteins. After incubation of recombinant proteins with erythrocytes, bound proteins were eluted from erythrocytes, with or without a wash with iRPMI, and detected in a blot by using anti-penta-His antibodies (Qiagen). ECTO was detected in an immunoblot of proteins eluted from unwashed erythrocytes, but not from washed erythrocytes, suggesting that unprocessed ECTO has a weak erythrocyte binding ability, and hence, the binding did not

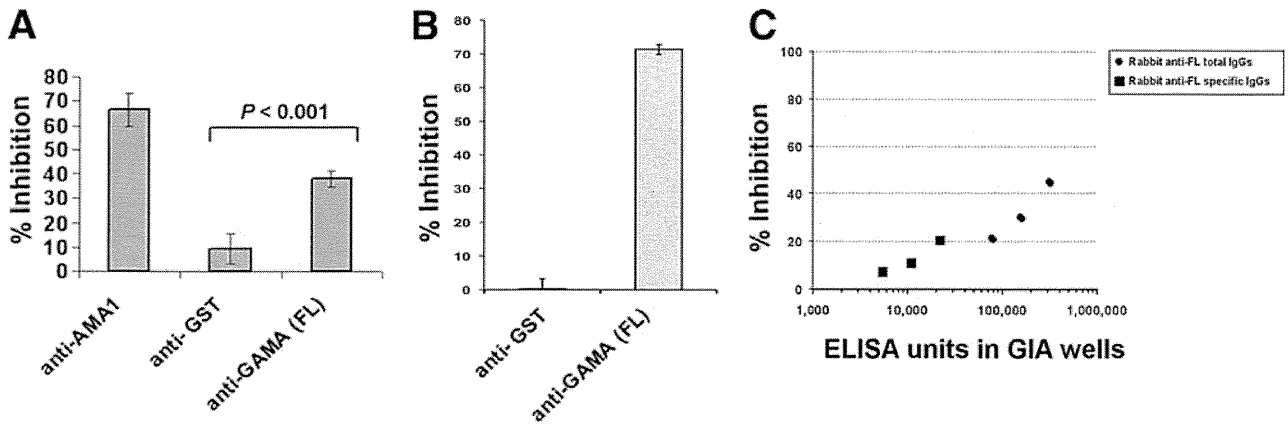

FIG. 4. Anti-FL antibody inhibits parasite invasion *in vitro*. (A) Anti-FL antibodies have invasion-inhibitory activity *in vitro*. The ability of the anti-FL antibodies to inhibit the parasite invasion into erythrocytes was tested in a one-cycle growth inhibition assay. Anti-AMA1 and anti-GST antibodies were used as positive and negative controls, respectively. The error bars represent the standard deviations of the means of the three independent experiments. One-way ANOVA was performed ($P < 0.001$) and followed by Bonferroni's pairwise multiple-comparison tests to compare anti-GST and anti-FL. (B) GAMA plays a role in the SA-independent invasion pathway. The ability of the anti-FL antibody to inhibit parasite invasion into neuraminidase-treated erythrocytes was tested in a one-cycle growth inhibition assay. Anti-GST antibody was used as a negative control. The bars represent the standard deviations of the means of the three independent experiments. (C) Anti-FL antibodies inhibit parasite invasion in a dose-dependent manner *in vitro*. The graph shows that the anti-FL antibodies, both total and antigen-specific IgGs, inhibited the invasion and/or growth in a dose-dependent manner in a one-cycle growth inhibition assay, as determined by measuring parasite LDH. The ELISA unit value was assigned as the reciprocal of the dilution giving an optical density (OD) at 415 nm equal to 1 in a standardized assay.

withstand a wash with iRPMI (Fig. 5A). When Tr1 and Tr3 were tested, only Tr3 and not Tr1 was detected in an immunoblot of proteins eluted both from unwashed and washed erythrocytes, suggesting that Tr3, not Tr1, has the erythrocyte binding ability and, hence, an erythrocyte binding epitope. The persistence of Tr3 binding even after erythrocytes were washed with iRPMI suggests that Tr3 has a stronger erythrocyte binding capacity than ECTO (Fig. 5A).

In order to verify whether Tr3 and native protein both bind a common receptor, the quantities of Tr3 in the proteins present in the blot of erythrocyte-bound proteins eluted from erythrocytes of either control (lane 1) and different treatments (lanes 2 through 5) were compared based on the measurement of band intensity by ImageJ analysis (Fig. 5B) (1). It showed that the quantity of Tr3 bound to erythrocytes that were preincubated with native GAMA was reduced by 50% (lane 5) relative to the control (lane 1), indicating that native GAMA preempts the receptors otherwise available for Tr3. However, there was no reduction in Tr3 quantity in other negative-control treatments (lane 2 to 4), indicating that neither GST nor Tr1 affects Tr3 binding. Similarly, in the reciprocal experiment, the quantity of native GAMA bound to erythrocytes that were preincubated with Tr3 was reduced by 50% (lane 7) relative to the control (lane 6), indicating that Tr3 preempts the receptors otherwise available for native GAMA (Fig. 5B). Taken together, these data show that native GAMA and Tr3 bind to the same receptor.

GAMA binds erythrocytes in a receptor-specific manner. The erythrocyte binding specificity of GAMA Tr3 was studied by testing the binding to enzyme-treated erythrocytes (Fig. 5C). Neuraminidase treatment of erythrocytes removes sialic acid (SA) residues in SA-containing erythrocyte receptors, and trypsin or chymotrypsin treatments differentially cleave the peptide backbones of erythrocyte receptors (33). The quantity of Tr3 protein detected in the immunoblot of proteins eluted from the surface of neuraminidase-treated erythrocytes was comparable to that of untreated erythrocytes. While the quantity of Tr3 eluted from trypsin-treated erythrocytes appeared to be only slightly reduced (15% reduction in signal intensity based on densitometry using Image J) (1), the quantity of Tr3 eluted from chymotrypsin-treated erythrocytes was much lower than that of untreated erythrocytes (85% reduction in signal intensity). The binding of native GAMA was resistant to neuraminidase and trypsin treatment but appeared sensitive to chymotrypsin treatment (35% reduction in signal intensity). As a control for enzyme treatments, EBA175 was also examined. As expected, EBA175 bound to erythrocytes in a neuraminidase-sensitive, trypsin-sensitive, and chymotrypsin-resistant manner (9). Taken together, these results suggest that GAMA binds a nonsialylated protein receptor.

GIA with neuraminidase-treated erythrocytes. The binding of GAMA to a nonsialylated protein receptor suggests that GAMA might be an invasion ligand that plays a role in the SA-independent invasion pathway. In order to verify this proposition, we tested parasite invasion into neuraminidase-treated erythrocytes in the presence of anti-GAMA antibodies and measured parasite growth over one cycle of replication by using flow cytometry. When anti-FL and anti-GST (negative control) IgGs were tested at final concentrations of 20 mg/ml, they inhibited invasion by 72% and 0.27%, respectively (Fig. 4B), suggesting that GAMA is a ligand that plays a role in the SA-independent invasion pathway.

Additive effects of antibodies in GIAs. It has been suggested that the presence of antibodies that target a broad range of invasion ligands (SA dependent and SA independent) involved in alternate invasion pathways would have greater growth-inhibitory activity (22). Since GAMA is an SA-independent ligand (that binds to neuraminidase-resistant, trypsin-resistant,

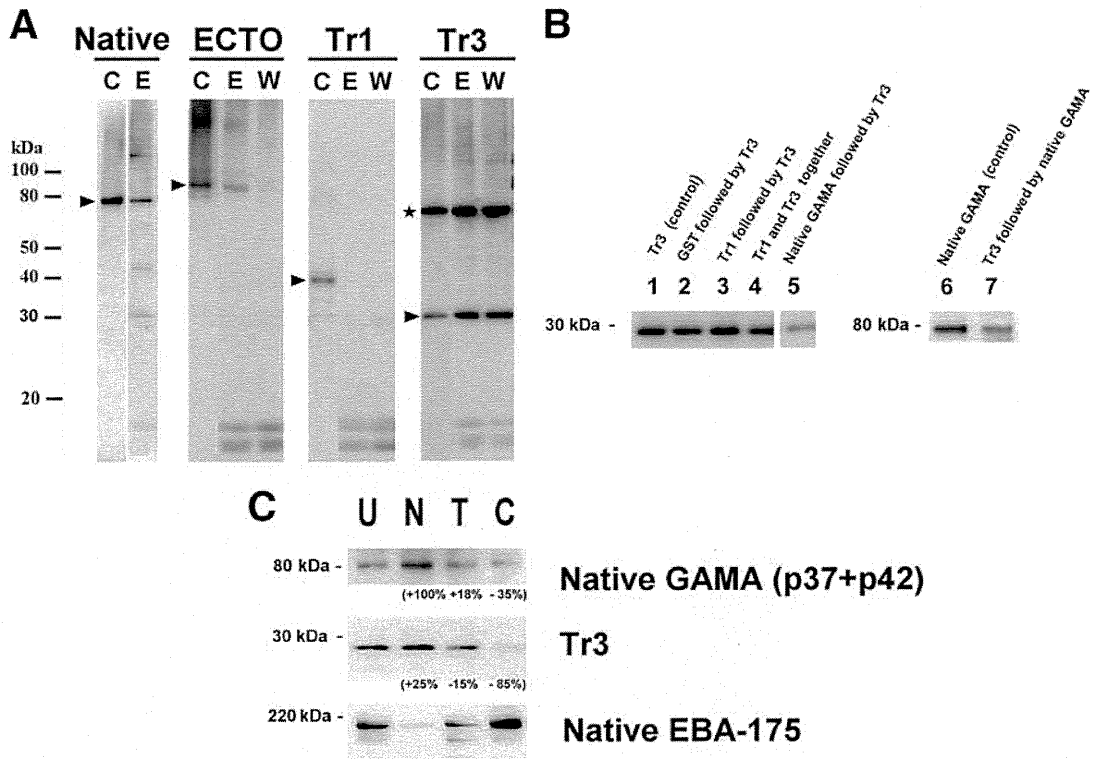

FIG. 5. Erythrocyte binding assay with native and recombinant GAMA. (A) Erythrocyte binding activities of native and recombinant GAMA proteins. The native GAMA protein in the culture supernatant or recombinant proteins (ECTO, Tr1, and Tr3) were incubated with human erythrocytes. The bound proteins were eluted with 0.5 M NaCl in PBS, pH 7.4, either directly from the incubated erythrocytes (E) or from the erythrocytes washed once with iRPMI (W). The eluted protein was detected by Western blotting either with rabbit anti-FL antibody (for GAMA) or with anti-penta-His antibodies (for ECTO, Tr1, and Tr3). For each experiment, the intact protein (without incubation or elution) was also detected by Western blotting as a control (C) (arrowheads). (Given that Tr3 has a cysteine residue, Tr3 forms an artificial homodimer [marked by an asterisk] with erythrocyte binding capacity.) (B) Tr3 competes for binding to a receptor(s) against native GAMA. The bands in lanes 1 through 5 and bands in lanes 6 and 7 refer to Tr3 and native GAMA, respectively, present in the blot of erythrocyte-bound proteins eluted from either controls or different treatments used in the binding assay (described above the lanes; also refer to Materials and Methods). Tr3 and native GAMA in the blot were detected with anti-penta-His and anti-FL antibodies, respectively. (C) GAMA binds erythrocytes in a receptor-specific manner. The erythrocyte binding abilities of native GAMA (present in the culture supernatant) and recombinant Tr3 were tested by incubation with untreated (U), neuraminidase-treated (N), trypsin-treated (T), and chymotrypsin-treated (C) erythrocytes, then elution with 0.5 M NaCl in PBS, pH 7.4, and detection by Western blotting with anti-penta-His (for Tr3) or anti-FL (for GAMA) antibodies. As a control for erythrocyte treatment, native EBA175 in the identical culture supernatant was also examined and detected by anti-EBA175 (regions 3 to 5) antibody. The values indicate percent changes in signal intensity of the relevant band relative to the band in lane U, calculated using Image J.

and chymotrypsin-sensitive erythrocyte receptors) (Fig. 5C) and EBA175 is an SA-dependent ligand (that binds to neuraminidase-sensitive, trypsin-sensitive, and chymotrypsin-resistant receptors) (Fig. 5C) (26), we were interested to test the first hypothesis, that a combination of anti-GAMA and anti-EBA175 antibodies may block both SA-dependent and SA-independent pathways and therefore exhibit a more potent invasion-inhibitory effect than either anti-GAMA or anti-EBA175 antibody alone.

Because of the colocalization of GAMA and AMA1 in free merozoites in our IFA, we were also interested to test the second hypothesis, that a combination of anti-GAMA and anti-AMA1 antibodies might exhibit a greater invasion-inhibitory effect than either anti-GAMA or anti-AMA1 antibody alone.

For testing of the two hypotheses described above, we did additive GIA experiments (Fig. 6). The following 6 antibody treatments were tried for inhibition of parasite growth over one cycle of replication with measurement of parasite growth by using flow cytometry: (i) anti-GST (negative control) (final concentration [fc], 20 mg/ml), (ii) anti-AMA1 (fc, 5 mg/ml), (iii) anti-EBA175 (regions 3 to 5) (fc, 1 mg/ml), (iv) anti-FL GAMA (fc, 15 mg/ml), (v) a mixture of anti-FL GAMA (fc, 15 mg/ml) and anti-AMA1 (fc, 5 mg/ml), and (vi) a mixture of anti-GAMA (fc, 15 mg/ml) and anti-EBA175 (regions 3 to 5) (fc, 1 mg/ml). The results (Fig. 6) showed that the invasion inhibition exhibited by the combination of anti-FL GAMA and anti-EBA175 antibodies was significantly greater (79%) than that by either anti-GAMA (41%) or anti-EBA175 (29%) alone. However, inhibition exhibited by the combination of anti-FL GAMA and anti-AMA1 antibodies (40%) was not significantly greater than that of either anti-GAMA (41%) or anti-AMA1 (35%) alone. The negative-control (anti-GST) antibodies inhibited invasion of 7%.

Reactivity of GAMA to human immune sera. Since GAMA is mobilized from the microneme onto the surface of merozo-

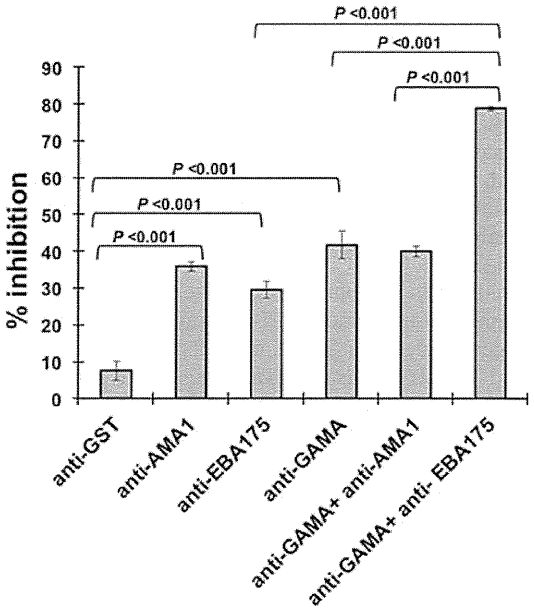

FIG. 6. Additive blocking of invasion. Antibodies, either separately or in combinations, were tested for inhibition of parasite invasion into erythrocytes in a one-cycle growth inhibition assay. Anti-GST antibody was used as a negative control (for concentrations of IgGs, refer to Results). The error bars represent the standard deviations of the means of the three independent experiments. One-way ANOVA was performed ($P < 0.001$) and followed by Bonferroni's pairwise multiple-comparison tests to compare each experimental group. Statistical significance between other groups was not tested.

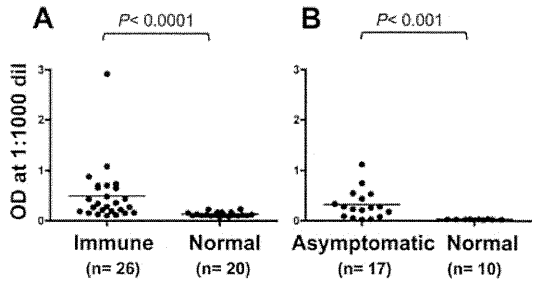

FIG. 7. Human sera from areas of malaria endemicity in Mali and Thai recognize GAMA in an ELISA. Probing of FL with sera from immune adults of Mali (Immune) and naive, nonexposed U.S. adults (Normal) (A) and with sera from *P. falciparum*-infected asymptomatic adults of Thai (Asymptomatic) and naive, nonexposed Thai adults (Normal) (B). The *P* values were calculated by Mann-Whitney *U* test. n indicates the number of sera analyzed. OD, optical density; dil, dilution.

ites (Fig. 3A) and anti-GAMA antibodies inhibited invasion *in vitro* (Fig. 4), we were interested to investigate whether GAMA is exposed to the human immune system in *P. falciparum*-infected individuals and generates an immune response. In order to test for the presence of anti-GAMA antibody in the sera, we tested sera from immune adults of Mali and West Africa and naive, nonexposed U.S. adults for antibodies to GAMA FL recombinant protein by ELISA (Fig. 7A) and sera from *P. falciparum*-infected asymptomatic adults of western Thailand and naive, nonexposed Thai adults for antibodies to GAMA FL recombinant protein (Fig. 7B). Sera of immune adults from Mali showed significantly higher reactivity to FL than those of malaria-naïve U.S. adults ($P < 0.0001$; Mann-Whitney *U* test) (Fig. 7A), and sera of asymptomatic Thai adults showed significantly higher reactivity to FL than those of malaria-naive Thai individuals ($P < 0.001$; Mann-Whitney *U* test) (Fig. 7B).

DISCUSSION

This study was performed with the objective of testing our hypothesis that GAMA may be a blood-stage vaccine candidate by using recombinant GAMA expressed in the wheat germ cell-free system.

Our Western blotting results (Fig. 2A) are in broad agreement with the previous findings (21) that primary and secondary processing events occur in GAMA. However, the detection of p37-p42 and the residual stub in our blot of parasite lysates, but not in that of the previous study (21), suggests that the secondary processing occurs prior to invasion and not at the time of invasion as described in the previous study. Our IEM results have confirmed for the first time that GAMA is indeed localized in micronemes of merozoites, and hence, GAMA represents a novel micronemal protein. It will be interesting to examine whether GAMA interacts with AMA1 or any other invasion-related merozoite proteins.

The GIA measures the capacity of antibodies to limit erythrocyte invasion and/or growth of *P. falciparum in vitro* (8). Our one-cycle GIA showed that anti-FL antibodies inhibited the merozoite invasion of erythrocytes. Similar assays using detection of parasitemia by parasite LDH assay also showed that anti-FL antibodies inhibited invasion and/or intraerythrocyte growth of the parasite in a dose-dependent manner. The two-cycle GIA showed that anti-FL, anti-Tr1, and anti-Tr3 antibodies inhibited invasion specifically.

Recently GAMA has been described as a novel erythrocyte binding protein (21). However, no recognizable protein motifs were identified in the primary structure of GAMA, and this raises the question of which regions of the protein are responsible for the demonstrated erythrocyte binding activity (21). In order to characterize the erythrocyte binding domain/epitope, truncated versions of GAMA were synthesized and tested for erythrocyte binding activity. Here, we have demonstrated that only Tr3, not Tr1, has the ability to bind erythrocytes, suggesting that the erythrocyte binding domain of GAMA resides in the C-terminal section of GAMA. Moreover, the binding of ECTO is weak, suggesting that while the unprocessed ECTO constrains the formation of proper erythrocyte binding domain in GAMA, processing of ECTO into the p37-p42 heterodimer is required for the facilitation of the formation and/or exposure of the erythrocyte binding domain. Our binding assays suggest that native GAMA and recombinant Tr3 bind to the same unknown receptor (Fig. 5B) and, importantly, revealed that the binding of native GAMA and Tr3 to human erythrocytes is neuraminidase resistant, SA independent, and chymotrypsin sensitive (Fig. 5C). However, it can be seen that the chymotrypsin treatment has a profound effect on binding of Tr3 rather than that of native GAMA. This may be due to the fact that Tr3 is a monomer and native GAMA is a heterodimer

with p37 and p42 fragments, and additionally, p37 in native GAMA might *per se* mediate interaction with a different receptor that is neuraminidase and chymotrypsin resistant. Identification of the GAMA receptor(s) in future studies will be important to understanding the binding specificities of GAMA. Taken together, these results indicate that GAMA binds a nonsialylated protein receptor, and hence, GAMA represents a novel SA-independent invasion ligand that plays a role in the SA-independent invasion pathway. Our results indicating that the invasion-inhibitory effect of anti-FL is more profound with neuraminidase-treated erythrocytes (i.e., 72%; Fig. 4B) than with untreated erythrocytes (i.e., 38%; Fig. 4A) validate that GAMA indeed plays a role in the SA-independent invasion pathway.

Invasion pathways can be broadly classified into 2 main groups based on the use of SA on the erythrocyte surface by parasite ligands (22): (i) SA-independent (neuraminidase-resistant) invasion (11, 31) and (ii) SA-dependent (neuraminidase-sensitive) invasion (5, 17, 23, 26). Therefore, we were interested in finding combinations of antigens that induce more-potent synergistic antiparasite activity. Our results (Fig. 6) indicating that a combination of antibodies against GAMA (an SA-independent ligand) and EBA175 (an SA-dependent ligand) exhibited a significantly greater invasion-inhibitory effect than either anti-GAMA or anti-EBA175 antibody alone support the rationale that, for achieving greater invasion inhibition, targeting of both SA-dependent and SA-independent ligands/pathways is better than targeting either of them alone. It will be worthwhile to further test whether a more potent, or possibly synergistic, antiparasitic activity can be achieved with either a combination vaccine (mixture of GAMA and EBA175 antigens) or a fusion vaccine (chimeric GAMA-EBA175 fusion protein) *in vivo*.

Based on the colocalization of GAMA and AMA1 (Fig. 3A), we also hypothesized that the combination of anti-GAMA and anti-AMA1 antibodies might exhibit a greater invasion-inhibitory effect than either of them alone. However, our results (Fig. 6) showed that it was not the case. Given that GAMA interacts with an unknown erythrocyte receptor and AMA1 interacts with RON2 (30), one of the plausible explanations for our result is that GAMA-erythrocyte receptor interaction might be upstream of the AMA1-RON2 interaction and blocking of GAMA-receptor interaction by anti-GAMA antibodies makes the downstream AMA1-RON2 interaction impossible and, hence, renders the inhibitory effect of anti-AMA1 antibody superfluous.

Immunoreactive antigens involved in erythrocyte invasion represent potential candidates for malaria vaccine development (10), and designing a vaccine based on sequences of immunoreactive antigens with minimum polymorphisms is critical to preventing the parasite from evading the vaccine-induced immunity. Our results indicating that GAMA is localized on the surface of free merozoite (Fig. 3A) and antibodies are generated against GAMA during natural infection in humans (Fig. 7) suggest that GAMA is an immunogenic antigen. In order to study whether GAMA is exposed to the host immune pressure, we compared the single nucleotide polymorphisms (SNPs) in GAMA of 12 laboratory strains (see Table S1 in the supplemental material) deposited in PlasmoDB (http://plasmodb.org/plasmo/). GAMA contains a total of 7 nonsynonymous SNPs, and importantly, there are only 4 nonsynonymous SNPs outside the long asparagine-rich region (residues 356 to 485 in Fig. 1A); 3 of them (at positions 67, 229, and 258) are in Tr1, and only 1 (at position 632) is in the Tr3 region (containing the erythrocyte binding epitope) of GAMA. These preliminary SNP analyses suggest that GAMA is less polymorphic and, hence, may be a promising blood-stage vaccine candidate antigen. However, to validate this claim, we need further analysis of SNPs of GAMA in different field isolates worldwide.

In contrast to peripheral merozoite surface proteins and other apical proteins, most GPI-anchored proteins are refractory to genetic deletion (28). Knockouts of the GAMA gene in 3D7 and W2mef strains of *P. falciparum* were attempted, but no GAMA gene deletion mutant could be generated (see Fig. S1 in the supplemental material), and thus we believe that GAMA is essential to *P. falciparum* parasite invasion. However, it can be seen that the genetic disruption of the GAMA ortholog was successful in *P. berghei* (12). This discrepancy may be due to the differences in host erythrocyte receptors. However, additional research is required to address this discrepancy.

In summary, our data establish that GAMA is an important micronemal antigen. The data indicating that GAMA is exposed to the human immune system and anti-GAMA antibodies block merozoite invasion of erythrocytes *in vitro* validate GAMA as a novel blood-stage vaccine candidate antigen and suggest that it may be a target of antibodies that contribute to acquired immunity to malaria. Erythrocyte binding assays revealed that GAMA possesses an erythrocyte binding epitope in the C-terminal region and it binds a nonsialylated protein receptor. Growth inhibition assays with neuraminidase-treated erythrocytes reveal that GAMA represents a ligand that plays a role in the SA-independent invasion pathway. The significantly greater invasion-inhibitory effect exhibited by the combination of anti-GAMA or anti-EBA175 antibodies supports the rationale that targeting of both SA-dependent and SA-independent ligands/pathways is better than targeting either of them alone. This study also substantiates that the wheat germ cell-free system is a valuable tool for identification of novel malaria vaccine candidates.

ACKNOWLEDGMENTS

We thank Masachika Shudo, Integrated Center for Science, Ehime University, Japan, for technical assistance. We also thank the Japanese Red Cross Society for providing us the human erythrocytes and human plasma.

This research was supported in part by grants from The Bill and Melinda Gates Foundation, from the Ministry of Education, Culture, Sports, Science and Technology (21249028, 21022034, 23406007, and 23117008), and from the Ministry of Health, Labor, and Welfare, Japan (H21-Chikyukibo-ippan-005). This study was supported in part by the intramural program of the National Institute of Allergy and Infectious Diseases/NIH, and the GIA Reference Center is supported by the PATH/Malaria Vaccine Initiative.

REFERENCES

1. **Abramoff, M. D., P. J. Magalhaes, and S. J. Ram.** 2004. Image processing with ImageJ. Biophotonics Int. **11**:36–42.
2. **Bei, A. K., et al.** 2010. A flow cytometry-based assay for measuring invasion of red blood cells by *Plasmodium falciparum*. Am. J. Hematol. **85**:234–237.
3. **Birkett, A. J.** 2010. PATH Malaria Vaccine Initiative (MVI): perspectives on the status of malaria vaccine development. Hum. Vaccin. **6**:139–145.

4. **Bozdech, Z., et al.** 2003. The transcriptome of the intraerythrocytic developmental cycle of *Plasmodium falciparum*. PLoS Biol. **1**:E5.
5. **Camus, D., and T. J. Hadley.** 1985. A *Plasmodium falciparum* antigen that binds to host erythrocytes and merozoites. Science **230**:553–556.
6. **Cao, J., et al.** 2009. Rhoptry neck protein RON2 forms a complex with microneme protein AMA1 in *Plasmodium falciparum* merozoites. Parasitol. Int. **58**:29–35.
7. **Coleman, R. E., et al.** 2004. Infectivity of asymptomatic *Plasmodium*-infected human populations to Anopheles dirus mosquitoes in western Thailand. J. Med. Entomol. **41**:201–208.
8. **Crompton, P. D., et al.** 2010. In vitro growth-inhibitory activity and malaria risk in a cohort study in Mali. Infect. Immun. **78**:737–745.
9. **Deans, A. M., et al.** 2007. Invasion pathways and malaria severity in Kenyan *Plasmodium falciparum* clinical isolates. Infect. Immun. **75**:3014–3020.
10. **Doolan, D. L., et al.** 2008. Profiling humoral immune responses to *P. falciparum* infection with protein microarrays. Proteomics **8**:4680–4694.
11. **Duraisingh, M. T., et al.** 2003. Phenotypic variation of *Plasmodium falciparum* merozoite proteins directs receptor targeting for invasion of human erythrocytes. EMBO J. **22**:1047–1057.
12. **Ecker, A., E. S. Bushell, R. Tewari, and R. E. Sinden.** 2008. Reverse genetics screen identifies six proteins important for malaria development in the mosquito. Mol. Microbiol. **70**:209–220.
13. **Florens, L., et al.** 2002. A proteomic view of the *Plasmodium falciparum* life cycle. Nature **419**:520–526.
14. **Fowkes, F. J., J. S. Richards, J. A. Simpson, and J. G. Beeson.** 2010. The relationship between anti-merozoite antibodies and incidence of *Plasmodium falciparum* malaria: a systematic review and meta-analysis. PLoS Med. **7**:e1000218.
15. **Gardner, M. J., et al.** 2002. Genome sequence of the human malaria parasite *Plasmodium falciparum*. Nature **419**:498–511.
16. **Genton, B.** 2008. Malaria vaccines: a toy for travelers or a tool for eradication? Expert Rev. Vaccines **7**:597–611.
17. **Gilberger, T. W., et al.** 2003. A novel erythrocyte binding antigen-175 paralogue from *Plasmodium falciparum* defines a new trypsin-resistant receptor on human erythrocytes. J. Biol. Chem. **278**:14480–14486.
18. **Gilson, P. R., et al.** 2006. Identification and stoichiometry of glycosylphosphatidylinositol-anchored membrane proteins of the human malaria parasite *Plasmodium falciparum*. Mol. Cell Proteomics **5**:1286–1299.
19. **Greenwood, B. M., et al.** 2008. Malaria: progress, perils, and prospects for eradication. J. Clin. Invest. **118**:1266–1276.
20. **Haase, S., et al.** 2008. Characterization of a conserved rhoptry-associated leucine zipper-like protein in the malaria parasite *Plasmodium falciparum*. Infect. Immun. **76**:879–887.
21. **Hinds, L., J. L. Green, E. Knuepfer, M. Grainger, and A. A. Holder.** 2009. Novel putative glycosylphosphatidylinositol-anchored micronemal antigen of *Plasmodium falciparum* that binds to erythrocytes. Eukaryot. Cell **8**:1869–1879.
22. **Lopaticki, S., et al.** 2011. Reticulocyte and erythrocyte binding-like proteins function cooperatively in invasion of human erythrocytes by malaria parasites. Infect. Immun. **79**:1107–1117.
23. **Maier, A. G., et al.** 2003. *Plasmodium falciparum* erythrocyte invasion through glycophorin C and selection for Gerbich negativity in human populations. Nat. Med. **9**:87–92.
24. **McCallum, F. J., et al.** 2008. Acquisition of growth-inhibitory antibodies against blood-stage *Plasmodium falciparum*. PLoS One **3**:e3571.
25. **Persson, K. E., C. T. Lee, K. Marsh, and J. G. Beeson.** 2006. Development and optimization of high-throughput methods to measure *Plasmodium falciparum*-specific growth inhibitory antibodies. J. Clin. Microbiol. **44**:1665–1673.
26. **Persson, K. E., et al.** 2008. Variation in use of erythrocyte invasion pathways by *Plasmodium falciparum* mediates evasion of human inhibitory antibodies. J. Clin. Invest. **118**:342–351.
27. **Richards, J. S., and J. G. Beeson.** 2009. The future for blood-stage vaccines against malaria. Immunol. Cell Biol. **87**:377–390.
28. **Sanders, P. R., et al.** 2006. A set of glycosylphosphatidyl inositol-anchored membrane proteins of *Plasmodium falciparum* is refractory to genetic deletion. Infect. Immun. **74**:4330–4338.
29. **Singh, K., et al.** 2010. Subdomain 3 of *Plasmodium falciparum* VAR2CSA DBL3x is identified as a minimal chondroitin sulfate A-binding region. J. Biol. Chem. **285**:24855–24862.
30. **Srinivasan, P., et al.** 2011. Binding of *Plasmodium* merozoite proteins RON2 and AMA1 triggers commitment to invasion. Proc. Natl. Acad. Sci. U. S. A. **108**:13275–13280.
31. **Stubbs, J., et al.** 2005. Molecular mechanism for switching of *P. falciparum* invasion pathways into human erythrocytes. Science **309**:1384–1387.
32. **Takeo, S., T. U. Arumugam, M. Torii, and T. Tsuboi.** 2009. Wheat germ cell-free technology for accelerating the malaria vaccine research. Expert Opin. Drug Discov. **4**:1191–1199.
33. **Tham, W. H., et al.** 2010. Complement receptor 1 is the host erythrocyte receptor for *Plasmodium falciparum* PfRh4 invasion ligand. Proc. Natl. Acad. Sci. U. S. A. **107**:17327–17332.
34. **Tsuboi, T., S. Takeo, T. U. Arumugam, H. Otsuki, and M. Torii.** 2010. The wheat germ cell-free protein synthesis system: a key tool for novel malaria vaccine candidate discovery. Acta Trop. **114**:171–176.
35. **Tsuboi, T., et al.** 2008. Wheat germ cell-free system-based production of malaria proteins for discovery of novel vaccine candidates. Infect. Immun. **76**:1702–1708.
36. **Tsuboi, T., S. Takeo, T. Sawasaki, M. Torii, and Y. Endo.** 2010. An efficient approach to the production of vaccines against the malaria parasite. Methods Mol. Biol. **607**:73–83.
37. **WHO.** 2010. World malaria report 2010. WHO Press, Geneva, Switzerland.
38. **Wilson, D. W., B. S. Crabb, and J. G. Beeson.** 2010. Development of fluorescent *Plasmodium falciparum* for in vitro growth inhibition assays. Malar. J. **9**:152.

Editor: J. H. Adams

Husain et al. BMC Genomics 2011, 12:275
http://www.biomedcentral.com/1471-2164/12/275

BMC Genomics

RESEARCH ARTICLE Open Access

Global analysis of gene expression in response to L-Cysteine deprivation in the anaerobic protozoan parasite *Entamoeba histolytica*

Afzal Husain[1,2], Ghulam Jeelani[1,3], Dan Sato[4] and Tomoyoshi Nozaki[1,5*]

Abstract

Background: *Entamoeba histolytica*, an enteric protozoan parasite, causes amebic colitis and extra intestinal abscesses in millions of inhabitants of endemic areas. *E. histolytica* completely lacks glutathione metabolism but possesses L-cysteine as the principle low molecular weight thiol. L-Cysteine is essential for the structure, stability, and various protein functions, including catalysis, electron transfer, redox regulation, nitrogen fixation, and sensing for regulatory processes. Recently, we demonstrated that in *E. histolytica*, L-cysteine regulates various metabolic pathways including energy, amino acid, and phospholipid metabolism.

Results: In this study, employing custom-made Affymetrix microarrays, we performed time course (3, 6, 12, 24, and 48 h) gene expression analysis upon L-cysteine deprivation. We identified that out of 9,327 genes represented on the array, 290 genes encoding proteins with functions in metabolism, signalling, DNA/RNA regulation, electron transport, stress response, membrane transport, vesicular trafficking/secretion, and cytoskeleton were differentially expressed (≥3 fold) at one or more time points upon L-cysteine deprivation. Approximately 60% of these modulated genes encoded proteins of no known function and annotated as hypothetical proteins. We also attempted further functional analysis of some of the most highly modulated genes by L-cysteine depletion.

Conclusions: To our surprise, L-cysteine depletion caused only limited changes in the expression of genes involved in sulfur-containing amino acid metabolism and oxidative stress defense. In contrast, we observed significant changes in the expression of several genes encoding iron sulfur flavoproteins, a major facilitator superfamily transporter, regulator of nonsense transcripts, NADPH-dependent oxido-reductase, short chain dehydrogenase, acetyltransferases, and various other genes involved in diverse cellular functions. This study represents the first genome-wide analysis of transcriptional changes induced by L-cysteine deprivation in protozoan parasites, and in eukaryotic organisms where L-cysteine represents the major intracellular thiol.

Background

L-Cysteine, a sulfur-containing amino acid (SAA), is ubiquitous in virtually all living organisms from bacteria to higher eukaryotes, and plays an essential role in the various cellular processes including stability, structure, regulation of catalytic activity, and posttranslational modification for various proteins. Due to the ability of its thiol group to undergo redox reactions, L-cysteine has antioxidant properties, and is used for the biosynthesis of glutathione, which is found in humans as well as other organisms. In addition, L-cysteine is also essential for the synthesis of trypanothione, coenzyme A, hypotaurine, taurine as well as ubiquitous iron-sulfur (Fe-S) clusters, which are involved in electron transfer, redox regulation, nitrogen fixation, and sensing for regulatory processes [1].

Entamoeba histolytica, an enteric protozoan parasite, causes amebic colitis and extra intestinal abscesses in millions of inhabitants of endemic areas, and responsible for thousands of deaths annually [2]. The trophozoites of *E. histolytica* primarily reside in the anaerobic environment of the colonic lumen, but are exposed to various reactive oxygen and nitrogen species (ROS and RNS) during tissue invasion, metastasis, and extra

* Correspondence: nozaki@nih.go.jp
[1]Department of Parasitology, National Institute of Infectious Diseases, 1-23-1 Toyama, Shinjuku, Tokyo 162-8640, Japan
Full list of author information is available at the end of the article

intestinal propagation [2,3]. *E. histolytica* lacks most of the components of the eukaryotic oxidative stress defence system including catalase, peroxidase, glutathione, and glutathione-recycling enzymes. However, it possesses alternative mechanisms for detoxification of the reactive oxygen and nitrogen species. The alternative mechanisms are most likely to involve superoxide dismutase (SOD), peroxiredoxin, flavodiiron proteins (FDPs), and reducing agents (thiols), especially L-cysteine [4-6]

Among a number of metabolic peculiarities, metabolism of SAAs in *E. histolytica* is distinct from that of its mammalian host in a variety of aspects. First, it lacks both forward and reverse trans-sulfuration pathways and thus is unable to interconvert L-methionine and L-cysteine [6] Second, it possesses methionine γ-lyase (MGL) which degrades L-methionine, L-homocysteine, and L-cysteine [7-9]. Third, *E. histolytica* possesses enzymes for the *de novo* S-methylcysteine/L-cysteine biosynthesis [10-12]. The S-methylcysteine/L-cysteine biosynthetic pathway involves serine acetyltransferase (SAT, EC2.3.1.30) that catalyzes acetyl CoA-dependent acetylation of the side chain hydroxyl group of L-serine to form O-acetylserine (OAS) [13]. Subsequently, cysteine synthase [(CS; OAS (thiol) lyase; EC4.2.99.8)] catalyzes the reaction of OAS with methanethiol or sulfide to produce S-methylcysteine or L-cysteine, respectively. Recombinant amebic CS isotypes possess both S-methylcysteine and L-cysteine synthesizing activities *in vitro*. However, our recent *in vivo* study [12] revealed that CS isotypes are primarily involved in the synthesis of SMC, but not of L-cysteine. Since, this pathway is not involved in the synthesis of L-cysteine, *in vitro* cultivation of amebic trophozoites requires high concentrations of L-cysteine, and this requirement can not be replaced by other thiols [14]. In *E. histolytica*, L-cysteine is required for the growth, attachment, survival, and protection from oxidative stress [14,15].

All prokaryotic and eukaryotic cells are known to have an ability to restructure their transcriptomes in order to adapt to the environmental conditions by sensing the endogenous level of various metabolites. Small-molecule metabolites, including amino acids, nucleotides, and carbohydrates have been shown to regulate the expression of large number of genes at the transcriptional and post-transcriptional levels [16]. In addition, intracellular redox determined by various metabolites has also been demonstrated to be an important regulator to gene expression [16].

In most eukaryotes, glutathione is the major thiol, and L-cysteine levels are maintained many fold lower than that of glutathione [17]. However, *E. histolytica* completely lacks glutathione metabolism and relies on L-cysteine as a major redox buffer [5, 6, and 8]. Therefore, *E. histolytica* represents an excellent model to study the effect of L-cysteine deprivation on gene expression and cellular metabolism. Our recent metabolomic study demonstrated that in *E. histolytica*, L-cysteine regulates various metabolic pathways, including energy, amino acid, and phospholipid metabolism [12]. In this study we performed DNA microarray analysis of gene expression in *E. histolytica* cultured in L-cysteine-deprived conditions. We found that the expression of a large number of genes was modulated in response to the L-cysteine deprivation.

Results and Discussions

L-Cysteine deprivation induces global changes in the gene expression

To better understand the role of L-cysteine in transcriptional regulation of gene expression in *E. histolytica*, we performed time course analysis of genome wide gene expression upon L-cysteine deprivation, using a custom-made Affymetrix microarray representing 9,327 of *E. histolytica* genes. We identified 290 genes (3.1%) modulated by at least 3 fold (p-value < 0.05) at one or more time points in response to L-cysteine deprivation (Additional file 1). Out of them, 129 genes were up-regulated and 167 genes were down-regulated, while 6 genes showed both up- and down-regulation depending upon the time points (Tables 1 and 2; Additional files 2 and 3). Out of the 129 up-regulated genes, 51 genes (40%) were assigned with putative biological functions, namely signalling, general metabolism, lipid metabolism, DNA/RNA regulation, electron transport, stress response, transport, and trafficking/secretion/cytoskeleton (Figure 1). The remaining 78 genes (60%) were categorized into genes encoding either hypothetical proteins without (68) or with known conserved domain(s) (10). A total of 167 genes were down regulated by ≥3 fold at one or more time points upon L-cysteine deprivation, 108 (65%) of which encode hypothetical proteins or hypothetical proteins containing conserved domain(s), whereas remaining 59 genes (35%) encode proteins with putative biological functions (Figure 1).

To verify the data obtained by Affymetrix-based microarray, we performed quantitative RT-PCR on five genes: two each from significantly up- (EHI_173950 and EHI_138480) and down-regulated genes (EHI_045340 and EHI_052890), respectively, and one invariant gene (EHI_056690), based on Affymetrix analysis. The results of qRT-PCR agreed well with the microarray data for all five transcripts tested (Table 3). The modulated genes were grouped into broad categories, based on the protein BLAST at NCBI and InterProScan at EMBL, and discussed below (Figure 1).

Table 1 List of most highly induced genes upon L-cysteine deprivation

Probe set ID	Accession numbers	Common Names	Basal Expression (log_2)	3 h	6 h	12 h	24 h	48 h	p value
EHI_173950_at	XM_647419	Major facilitator superfamily (MFS) transporter	6.11	+ 4.1	+ 14.6	+ 10.0	+ 4.7	+ 2.6	3.0E-07
EHI_138480_at	XM_650038	Iron-sulfur flavoprotein, putative	8.40	+ 3.6	+ 6.8	+ 9.8	+ 5.4	+ 4.2	4.5E-08
EHI_025710_at	XM_644279	Iron-sulfur flavoprotein, putative	7.17	+ 3.6	+ 5.4	+ 8.7	+ 5.2	+ 3.9	1.0E-06
13.m00350_at	XM_651312	Hypothetical protein	2.73	- 1.0	+ 2.4	+ 7.8	+ 5.4	+ 6.5	2.4E-04
EHI_176810_at	XM_644746	Hypothetical protein	3.53	+ 4.8	+ 8.8	+ 6.0	+ 1.2	- 1.3	4.6E-04
EHI_130490_at	XM_643338	Hypothetical protein	7.42	+ 1.7	+ 1.9	+ 5.8	+ 3.5	+ 1.7	1.8E-05
EHI_091050_at	XM_645468	Zinc finger protein, putative (IBR superfamily)	5.39	+ 2.9	+ 9.1	+ 5.7	- 1.4	- 1.7	1.3E-06
EHI_080280_at	XM_644430	Glu6-phosphate N-acetyltransferase. putative	3.79	+ 8.6	+ 6.2	+ 5.5	+ 1.3	- 1.3	3.3E-05
EHI_032670_s_at	XM_645799	Iron sulfur flavoprotein like, putative	7.47	+ 1.5	+ 3.5	+ 5.4	+ 3.9	+ 4.0	3.4E-06
870.m00013_x_at	XM_642792	Hypothetical protein	2.54	+ 3.4	+ 6.4	+ 5.0	+ 1.3	+ 1.9	6.5E-04
EHI_096770_at	XM_650580	Acetyltransferase, putative	7.01	+ 1.9	+ 3.4	+ 4.8	+ 3.7	+ 4.2	4.9E-05
EHI_137260_at	XM_647486	Hypothetical protein	2.97	+ 3.7	+ 4.4	+ 4.8	+ 2.4	+ 2.6	2.0E-03
65.m00145_x_at	XM_648920	Hypothetical protein	3.08	+ 1.2	+ 3.3	+ 4.7	+ 1.1	- 1.6	6.1E-06
EHI_062300_at	XM_645096	Hypothetical protein	4.10	+ 1.7	+ 1.9	+ 4.7	+ 2.7	+ 2.1	1.7E-03
337.m00049_x_at	XM_644075	Hypothetical protein	2.48	+ 2.9	+ 5.2	+ 4.5	+ 1.7	+ 1.0	1.5E-03
EHI_148740_at	XM_001913345	Hypothetical protein	8.19	+ 1.9	+ 2.7	+ 4.4	+ 1.7	+ 1.3	1.0E-06
79.m00141_x_at	XM_648476	Hypothetical protein	2.90	+ 2.0	+ 3.1	+ 4.4	+ 1.7	+ 1.2	2.4E-02
EHI_189190_x_at	XM_644225	Hypothetical protein	3.25	+ 1.7	+ 4.8	+ 4.4	- 1.0	- 1.9	4.3E-05
EHI_039720_at	XM_642957	Hypothetical protein	2.53	- 1.0	+ 2.1	+ 4.4	+ 3.3	+ 1.4	1.6E-05
EHI_051040_s_at	XM_647890	Hypothetical protein	6.82	+ 1.5	+ 2.7	+ 4.4	+ 2.5	+ 2.8	1.9E-03
EHI_139080_at	XM_643428	Longevity-assurance family protein	5.38	- 2.3	+ 1.2	+ 4.4	+ 2.3	+ 2.0	4.4E-06
EHI_067230_x_at	XM_647567	Hypothetical protein	6.18	+ 9.7	+ 13.6	+ 4.2	- 1.3	- 1.1	1.4E-07
EHI_055680_at	XM_646949	Heat shock protein, Hsp20 family, putative	5.63	+ 2.0	+ 4.6	+ 4.2	+ 1.6	+ 1.2	1.4E-03
EHI_086500_s_at	XM_646060	Short chain dehydrogenase	4.86	+ 6.1	+ 8.1	+ 4.2	+ 1.1	- 1.4	1.2E-04
EHI_148970_s_at	XM_652477	Regulator of nonsense transcripts, putative	9.86	+ 5.9	- 1.0	- 4.1	- 5.1	- 9.7	1.5E-07
EHI_139090_at	XM_643429	Hypothetical protein	5.95	+ 1.6	+ 1.9	+ 4.1	+ 1.3	- 1.5	6.2E-05
167.m00129_at	XM_646319	Hypothetical protein	3.36	+ 2.4	+ 4.8	+ 4.0	+ 2.0	+ 1.9	1.6E-03
EHI_110840_s_at	XM_649191	Regulator of nonsense transcripts, putative	9.73	+ 6.5	+ 1.0	- 4.0	- 4.6	- 8.7	1.2E-07
EHI_178130_at	XM_646412	Hypothetical protein	5.09	+ 2.0	+ 3.2	+ 4.0	+ 2.4	+ 2.8	5.9E-05
EHI_110370_at	XM_651955	Hypothetical protein	4.52	- 1.3	+ 1.3	+ 3.9	+ 2.6	+ 4.1	2.0E-04
EHI_070810_x_at	XM_649317	Regulator of nonsense transcripts, putative	4.76	+ 7.4	- 1.1	- 3.9	- 4.3	- 4.8	1.6E-05
EHI_004990_at	XM_647768	Ankyrin, putative	6.30	+ 2.0	+ 4.3	+ 3.8	+ 2.4	+ 3.0	5.1E-05
EHI_023330_at	XM_650547	Hypothetical protein	9.16	+ 6.5	+ 1.4	- 3.6	- 7.1	- 8.3	8.2E-07
EHI_005160_s_at	XM_647757	Hypothetical protein	2.94	+ 2.9	+ 4.5	+ 3.4	+ 1.6	+ 1.2	6.7E-03
EHI_028940_at	XM_647571	Hypothetical protein	8.44	+ 6.1	+ 6.5	+ 3.4	- 1.0	- 1.2	1.4E-07
EHI_033240_x_at	XM_645809	Riboflavin kinase/FAD synthetase, putative	6.61	+ 1.4	+ 4.6	+ 3.4	+ 3.0	+ 2.6	8.6E-07
493.m00030_x_at	XM_643175	Hypothetical protein	8.73	+ 3.9	+ 5.2	+ 3.3	- 1.8	- 1.9	1.4E-07
15.m00356_at	XM_651173	Hypothetical protein	7.03	+ 3.4	+ 4.2	+ 3.3	+ 1.7	+ 2.1	1.8E-03
EHI_110480_at	XM_651901	Hypothetical protein	4.51	+ 2.3	+ 4.2	+ 3.3	+ 2.9	+ 1.7	1.5E-04
EHI_140620_x_at	XM_645555	Hypothetical protein	2.32	+ 2.1	+ 5.9	+ 3.2	+ 1.3	+ 1.2	2.3E-02
EHI_136430_at	XM_650171	Hypothetical protein	4.08	+ 7.5	+ 7.8	+ 3.2	- 2.3	+ 1.0	4.1E-06
373.m00052_s_at	XM_643804	Hypothetical protein	6.53	+ 4.1	+ 2.0	+ 3.1	+ 1.0	- 1.1	7.9E-04
EHI_141030_at	XM_649510	DNA methyltransferase, putative	5.97	+ 2.4	+ 1.7	+ 2.3	+ 3.9	+ 4.1	3.6E-05
EHI_178520_at	XM_647939	Regulator of nonsense transcripts, putative	6.30	+ 6.2	- 1.4	- 2.1	- 1.9	- 1.4	8.7E-06
EHI_142270_at	XM_648119	Hypothetical protein	8.27	+ 3.7	+ 4.1	+ 2.0	- 1.0	- 1.1	2.9E-04
EHI_014340_at	XM_649988	Hypothetical protein	6.45	+ 2.7	+ 5.2	+ 1.9	+ 1.1	- 1.1	4.9E-05
EHI_064440_at	XM_648922	Hypothetical protein	5.03	- 1.5	- 1.2	+ 1.7	+ 2.5	+ 4.0	2.0E-03
EHI_120930_s_at	XM_649257	Protein kinase domain containing protein	2.61	+ 6.8	- 1.0	+ 1.5	+ 2.3	+ 1.8	2.4E-03

Table 1 List of most highly induced genes upon L-cysteine deprivation *(Continued)*

637.m00013_s_at	XM_642916	Regulator of nonsense transcripts, putative	2.92	+ 6.6	- 1.2	- 1.5	- 1.5	- 1.1	3.6E-05
EHI_031640_at	XM_648447	Hypothetical protein	6.98	+ 2.3	- 3.1	+ 1.5	+ 3.6	+ 5.8	1.8E-06
EHI_103640_at	XM_643960	Protein kinase domain containing protein	3.10	+ 5.2	- 1.0	- 1.4	+ 1.4	+ 1.2	5.6E-04
EHI_014910_s_at	XM_001914428	Hypothetical protein	2.99	+ 6.0	+ 1.5	- 1.3	+ 1.4	- 1.2	2.7E-04
EHI_038910_at	XM_651787	Hypothetical protein	2.57	+ 5.3	+ 2.3	+ 1.2	+ 1.6	- 1.0	5.1E-03
EHI_190460_at	XM_646352	Amino acid transporter, putative	3.11	- 1.2	- 1.4	+ 1.2	+ 2.2	+ 3.9	2.9E-03
EHI_084710_at	XM_650002	Hypothetical protein	4.27	+ 5.3	+ 2.3	+ 1.1	+ 2.2	+ 1.2	5.1E-04
EHI_054680_at	XM_646972	Hypothetical protein	3.09	- 1.2	- 1.4	- 1.1	+ 2.7	+ 5.9	4.8E-04
50.m00196_s_at	XM_649450	Hypothetical protein	4.95	+ 4.2	- 1.5	- 1.1	+ 1.2	- 1.4	9.0E-05
EHI_046040_s_at	XM_645992	Hypothetical protein	5.08	+ 6.5	+ 1.5	- 1.1	- 1.0	- 1.6	1.1E-05

The probe set IDs, accession numbers, common names, basal expressions, fold changes, and p values of most highly induced genes upon L-cysteine deprivation are shown.

Effect of L-cysteine deprivation on SAA metabolism

To further explore the role of L-cysteine in the regulation of expression of genes involved in SAA metabolism and associated pathways, we investigated their expression upon L-cysteine deprivation. As shown in Figure 2A, most of the genes involved in SAA metabolism except phosphoserine aminotransferase (PSAT) were not modulated by >3 fold upon L-cysteine deprivation. PSAT, an enzyme that catalyzes the reversible conversion of 3-phosphohydroxypyruvate to L-phosphoserine, the second step of phosphorylated L-serine biosynthetic pathway, was down-regulated by 3.3 fold at 48 h (Figure 2B). Other genes that were slightly modulated by L-cysteine deprivation included methionine adenosyltransferase (MAT) and phosphoglycerate dehydrogenase (PGDH), which were induced by >2 fold at early (3-6 h) and late (24-48 h) time points of L-cysteine deprivation, respectively (Figure 2B). This lack of changes in the expression of genes involved in SAA metabolism might be due to their high basal expression (except CS3 and SAT2, which have relatively low expression) under normal conditions(Additional file 4). Alternatively, it may be because L-cysteine has a very limited influence on the expression of the genes involved in SAA metabolism in *E. histolytica*. However, L-cysteine has been shown to significantly modulate the metabolic flux across SAA metabolism in *E. histolytica* [12]. In contrast to *E. histolytica*, L-cysteine availability is known to have a significant influence on the expression of the genes involved in SAA metabolism in other eukaryotic cells [18]. For example, in HepG2/C3A cells, L-cysteine deprivation resulted in the induction of cysteinyl-tRNA synthetase, glutamate-cysteine ligase, L-cystine-glutamate transporter, cystathionine γ-lyase, and glutamate-cysteine ligase, and a down-regulation of 3-phosphoadenosine 5-phosphosulfate synthase and sulfite oxidase [18].

We have recently shown by metabolomic analysis that the synthesis of OAS and SMC markedly increased upon L-cysteine deprivation in *E. histolytica*. OAS in bacteria is known to regulate the genes of cysteine regulon, and increment in its level modulates the expression of the genes involved in L-cysteine and sulfide synthesis [19]. However, no such regulation of genes of cysteine biosynthetic pathway was observed in *E. histolytica*, except a 2 fold down-regulation of a gene encoding SAT2, and slight induction of a gene encoding SAT3 (Figure 2B). These results imply that L-cysteine does not significantly modulate expression of the genes involved in SAA metabolism in *E. histolytica*; however, it affects the flux of SAA metabolism by post-transcriptional or post-translational mechanisms.

Effect of L-cysteine deprivation on the genes involved in oxidative and nitrosative stress defense

The *E. histolytica* genome contains several genes encoding ROS and RNS detoxifying proteins, such as peroxiredoxin, rubrerythrin, hybrid-cluster protein, superoxide dismutase (SOD), and flavodiiron proteins (FDPs) [6]. FDPs are widespread in prokaryotes, and known to be involved in the reduction of oxygen and/or nitric oxide whereas peroxiredoxin, rubrerythrin, hybrid-cluster protein, and superoxide dismutase (SOD) are involved in the detoxification of H_2O_2 and/or superoxide radicals [20-22]. Although L-cysteine deprivation led to the increment in the level of intracellular ROS [12], the genes encoding putative ROS-and RNS-detoxifying proteins in *E. histolytica* were not significantly modulated (Figure 3A). This is consistent with the previous studies that genes encoding known ROS and RNS detoxification pathways are not modulated in response to H_2O_2-mediated oxidative or DPTA-NONOate-mediated nitrosative stress in *E. histolytica* [23]. The lack of induction of the genes involved in oxidative/nitrosative stress is likely due to their high baseline expression even in the absence of oxidative or nitrosative stress. While most of the known genes in the ROS and RNS detoxification pathways were not modulated, one (EHI_129890) of the four FDP genes was slightly (up to 2.6 fold) up-regulated

Table 2 List of most highly down-regulated genes upon L-cysteine deprivation

Probe set ID	Accession numbers	Common Names	Basal Expression (log_2)	3h	6h	12h	24h	48h	p value
72.m00179_at	XM_648717	Hypothetical protein	8.8	+ 1.1	+1.4	- 2.8	- 15.3	- 22.8	2.5E-06
EHI_045340_s_at	XM_648481	NADPH-dependent oxidoreductase (EhNO2)	10.6	- 1.9	-1.9	- 3.0	- 10.6	- 8.3	1.4E-07
EHI_023330_at	XM_650547	Hypothetical protein	9.2	+ 6.5	+1.4	- 3.6	- 7.1	- 8.3	8.2E-07
EHI_148970_s_at	XM_652477	Regulator of nonsense transcripts, putative	9.9	+ 5.9	-1.0	- 4.1	- 5.1	- 9.7	1.5E-07
EHI_110840_s_at	XM_649191	Regulator of nonsense transcripts, putative	9.7	+ 6.5	+1.0	- 4.0	- 4.6	- 8.7	1.2E-07
EHI_070810_x_at	XM_649317	Regulator of nonsense transcripts, putative	4.8	+ 7.4	-1.1	- 3.9	- 4.3	- 4.8	1.6E-05
EHI_049960_at	XM_651359	Hypothetical protein	7.8	+ 2.4	-1.6	- 5.1	- 3.3	- 2.9	5.1E-07
EHI_182260_s_at	XM_001914319	Cysteine protease, putative	7.8	- 1.7	-3.2	- 2.5	- 3.2	- 6.3	2.7E-05
EHI_052890_at	XM_645369	Hypothetical protein	9.0	- 1.1	-6.3	- 11.1	- 3.0	- 2.6	3.5E-05
EHI_077280_s_at	XM_649853	Leucine rich repeat protein, BspA family	8.4	- 5.4	-6.7	- 2.2	- 2.7	- 1.1	2.5E-03
EHI_178790_at	XM_651153	Hypothetical protein	4.7	- 1.7	-5.1	- 1.6	+ 2.5	+ 3.0	1.2E-04
EHI_094060_s_at	XM_001913553	Actin binding protein, putative	9.2	+ 1.3	-3.5	- 5.0	- 2.5	- 3.2	1.8E-03
371.m00031_s_at	XM_643815	Leucine rich repeat protein	8.3	- 4.3	-3.2	- 2.4	- 2.4	- 1.4	1.5E-02
EHI_049570_at	XM_650791	RhoGAP domain containing protein	6.9	+ 2.1	-2.3	- 5.0	- 2.3	- 2.6	8.7E-04
EHI_130710_at	XM_644068	Myb-like DNA-binding protein	6.3	+ 1.3	-1.9	- 4.4	- 2.2	- 1.9	1.6E-05
EHI_197440_at	XM_646593	Hypothetical protein	10.6	+ 1.5	-2.7	- 4.1	- 1.9	- 2.6	1.0E-03
330.m00075_x_at	XM_644126	Hypothetical protein	6.9	+ 1.1	+1.0	- 3.3	+ 1.8	- 7.2	1.9E-03
EHI_148650_at	XM_652381	Leucine rich repeat/phosphatase domain containing protein	7.2	- 2.4	-4.5	- 2.9	- 1.7	- 1.6	1.2E-03
EHI_050660_at	XM_651502	Hypothetical protein	7.3	+ 1.7	-3.7	- 4.4	- 1.7	- 1.6	8.1E-04
EHI_044890_at	XM_652115	Helicase, putative	5.6	- 1.0	-4.3	- 2.3	- 1.6	- 1.4	6.5E-03
49.m00187_x_at	XM_649517	Fatty acid elongase, putative	4.8	+ 1.3	-5.6	- 5.4	- 1.6	- 1.7	3.3E-05
EHI_094780_s_at	XM_001914195	Pescadillo homolog, putative	5.7	+ 1.4	-2.9	- 4.0	- 1.6	- 2.1	8.5E-03
260.m00059_s_at	XM_644821	Phospholipase D like protein	4.4	+ 1.7	-3.6	- 4.2	- 1.6	- 3.0	2.1E-03
EHI_140530_at	XM_649099	Hypothetical protein	4.9	+ 1.4	-2.3	- 4.5	+ 1.6	+ 1.3	1.1E-04
EHI_145850_at	XM_650629	Hypothetical protein	4.9	+ 1.1	-3.2	- 5.8	- 1.5	- 2.0	2.3E-03
EHI_046630_at	XM_645444	Rho family GTPase	6.0	- 1.1	-4.4	- 4.4	+ 1.5	- 1.2	2.2E-04
EHI_187100_at	XM_651384	Hypothetical protein	6.9	- 1.3	-4.4	- 2.4	- 1.5	- 1.1	2.5E-06
849.m00008_s_at	XM_642804	Leucine rich repeat protein	7.9	- 5.1	-3.5	- 2.1	- 1.5	- 1.1	1.4E-02
EHI_009840_s_at	XM_652013	Hypothetical protein	11.1	- 4.3	-1.2	+ 1.4	+ 1.5	+ 1.6	4.0E-07
EHI_039330_at	XM_648669	Hypothetical protein	9.3	+ 1.1	-4.3	- 2.9	- 1.5	- 1.4	2.6E-02
266.m00066_s_at	XM_644755	Hypothetical protein	7.1	+ 1.6	+1.0	- 1.3	+ 1.4	- 6.6	1.3E-05
EHI_029500_s_at	XM_644980	Hypothetical protein	6.9	+ 1.7	-1.0	- 1.4	+ 1.4	- 7.4	1.6E-04
216.m00082_x_at	XM_645403	Hypothetical protein	6.0	- 2.3	-4.1	- 3.9	- 1.4	- 1.8	4.4E-04
EHI_196770_s_at	XM_001914173	Leucine rich repeat protein	8.2	- 3.4	-4.6	- 2.1	- 1.3	+ 1.0	2.9E-02
EHI_034590_s_at	XM_001914026	Hypothetical protein	7.1	+ 1.2	-1.2	- 1.4	+ 1.3	- 6.4	5.2E-05
EHI_107660_at	XM_644692	Hypothetical conserved, protein	9.1	- 5.7	-2.0	+ 1.1	+ 1.3	+ 1.7	1.1E-06
207.m00059_x_at	XM_645533	Actinin-like protein, putative	5.4	+ 1.7	-5.4	- 2.4	- 1.3	- 1.6	6.4E-03
EHI_182540_at	XM_651612	Hypothetical protein	6.3	+ 1.0	-3.2	- 4.1	+ 1.3	- 1.0	5.4E-04
EHI_010130_at	XM_651999	Hypothetical protein	6.6	- 9.5	-5.3	- 1.3	- 1.3	- 1.1	4.0E-06
EHI_018030_s_at	XM_001914259	Hypothetical protein	7.1	+ 1.4	+1.0	- 1.1	+ 1.3	- 11.0	4.3E-05
EHI_020830_s_at	XM_001913952	Hypothetical protein	9.4	+ 1.4	-1.3	- 1.2	+ 1.3	- 9.9	1.4E-05
EHI_002240_s_at	XM_645752	Hypothetical protein	7.1	+ 1.4	-1.0	- 1.2	+ 1.2	- 6.6	1.9E-04
EHI_196760_s_at	XM_643708	Hypothetical protein	9.4	+ 1.5	-1.3	- 1.2	+ 1.2	- 8.4	1.0E-05
EHI_037700_s_at	XM_643865	Hypothetical protein	7.1	+ 1.4	-1.1	- 1.3	+ 1.2	- 7.0	3.3E-05
EHI_189540_x_at	XM_645163	Hypothetical protein	5.0	+ 1.5	-4.1	- 2.4	- 1.2	- 2.1	9.9E-03
EHI_196720_s_at	XM_643106	Hypothetical protein	7.1	+ 1.5	-1.1	- 1.3	+ 1.2	- 10.1	2.8E-04
375.m00058_s_at	XM_643788	Hypothetical protein	7.1	+ 1.5	-1.1	- 1.3	+ 1.2	- 6.3	2.6E-04
194.m00101_s_at	XM_645779	Hypothetical protein	7.2	+ 1.4	-1.1	- 1.4	+ 1.2	- 6.9	8.0E-05
372.m00048_s_at	XM_643812	Protein kinase domain containing protein	6.0	+ 1.1	-4.0	- 4.0	+ 1.1	- 1.1	1.8E-04

Table 2 List of most highly down-regulated genes upon L-cysteine deprivation *(Continued)*

EHI_144150_s_at	XM_001914451	Hypothetical protein	6.3	+ 1.8	-1.6	- 2.0	+ 1.1	- 13.2	1.5E-04
EHI_020840_s_at	XM_001913953	Hypothetical protein	7.4	+ 1.7	-1.4	- 1.9	- 1.1	- 18.9	4.1E-05
EHI_103840_at	XM_648260	DNA repair protein, putative	6.1	+ 1.2	-3.1	- 4.3	+ 1.0	- 1.1	3.1E-03
506.m00025_s_at	XM_643137	Hypothetical protein	8.3	+ 1.1	-1.0	- 1.9	- 1.0	- 6.8	9.9E-04
390.m00061_s_at	XM_643707	Hypothetical protein	7.4	+ 1.7	-1.5	- 1.7	- 1.0	- 12.6	1.1E-05
EHI_145330_s_at	XM_001913871	Hypothetical protein	6.5	+ 1.2	-1.1	- 1.8	- 1.0	- 6.5	5.1E-05
EHI_099250_at	XM_649200	Hypothetical protein	6.3	+ 1.2	-1.9	- 4.0	- 1.0	- 1.3	2.1E-04
EHI_196770_s_at	XM_001914173	Hypothetical protein	7.4	+ 1.8	-1.4	- 1.5	- 1.0	- 17.1	2.7E-05
190.m00086_s_at	XM_645857	Hypothetical protein	8.4	+ 1.0	-1.1	- 2.0	- 1.0	-6.4	1.1E-03

The probe set IDs, accession numbers, common names, basal expressions, fold changes, and p values of most highly down-regulated genes upon L-cysteine deprivation are shown.

upon L-cysteine deprivation (Figure 3A). These findings suggest that *E. histolytica* might employ other post-transcriptional or post-translational regulatory mechanisms, such as RNA transport, protein modifications, allosteric regulations, and redirection of metabolic fluxes, to cope up with the oxidative stress.

The comparison of the genes modulated in response to L-cysteine deprivation with those modulated upon oxidative or nitrosative stress showed a very limited overlap (Figure 3B). Genes modulated upon L-cysteine deprivation shared only 27 or 31 genes with those modulated by oxidative or nitrosative stress, respectively (Figure 3B). Of these shared genes, 17 genes were shared by all the three conditions, suggesting that these genes play a general (or central) role in the response against L-cysteine deprivation and oxidative/nitrosative stress. A list of these shared genes is shown in Additional file 5. Among the genes that were up-regulated by L-cysteine deprivation and oxidative/nitrosative stress were several genes encoding iron sulfur flavoproteins (ISF) (EHI_067720, EHI_025710, EHI_138480). Interestingly, ISFs were among the most highly up-regulated genes by L-cysteine deprivation. ISFs constitute a widespread family of redox-active proteins found predominantly in anaerobic prokaryotes [24]. They are flavin mononucleotide (FMN) cofactor, and iron-sulfur [Fe-S] clusters containing proteins with an unusually compact cysteine motif [25]. The deduced amino acid sequences of amebic ISFs also suggest the presence of this compact cysteine motif (CX2CX2CX5-7C) that is most likely involved in the ligation of [4Fe-4S] clusters [25,26].

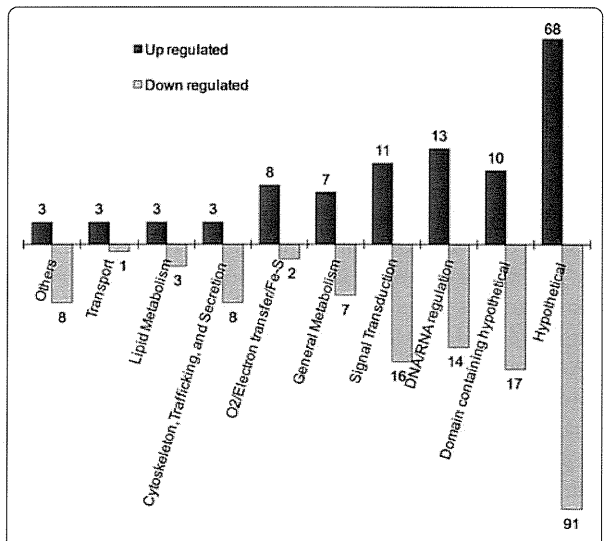

Figure 1 Functional distribution of differentially expressed genes upon L-cysteine deprivation. Genes were grouped according to putative functions inferred from the respective annotations. The exact number of changed transcripts is shown beside each column.

Iron sulfur flavoproteins belong to a novel family of proteins that are widely distributed in distantly related anaerobic prokaryotes. Interestingly, *E. histolytica* and *Trichomonas vaginalis* are the only members of the domain *Eukarya* that possess ISFs [6, 26]. There are at least 7 independent genes for ISFs in the genome of *E. histolytica*. However, the total number entries in *E. histolytica* database representing ISF genes is 13 as some of the sequences show very high mutual sequence identities (95-99%). A total of 7 probe sets representing 5 different ISF genes were up regulated ≥3 fold at one or more time points upon L-cysteine deprivation (Figure 4). Two of these ISF genes (EHI_138480 and EHI_025710) showed a maximum induction of 9.8 and 8.7 fold at 12 h of L-cysteine deprivation, respectively. The remaining probe sets were induced by only 3-6 folds upon L-cysteine deprivation. Three ISF genes, including two ISF genes highly induced upon L-cysteine deprivation (EHI_138480 and EHI_025710), were also induced by oxidative stress [23]. In contrast to their induction in response to L-cysteine deprivation or oxidative stress, two ISF genes (EHI_067720, EHI_134740) were down-regulated by 2-5 folds on day 1 and day 29 in the mouse model of intestinal amoebiasis [27]. These findings suggest that the expression of ISFs is regulated

Table 3 Verification of the microarray data by qRT-PCR

Common Name	Accession Number	Fold Change				
		3 h	6 h	12 h	24 h	48 h
Major fascilitator superfamily (MFS) transporter	XM_647419	2.0	12.8	7.2	4.2	2.3
		(4.1)	(14.6)	(9.9)	(4.7)	(2.6)
Iron sulfur flavoprotein (ISF)	XM_650038	1.8	4.4	14.9	5.5	2.8
		(3.6)	(6.8)	(9.8)	(5.4)	(4.2)
NADPH-dependent oxidoreductase (EhNO2)	XM_648481	-3.0	-3.0	-6.0	-8.4	-7.8
		(-1.9)	(-1.9)	(-3.0)	(-10.6)	(-8.3)
Hypothetical protein	XM_645369	-2.2	-6.4	-12.9	-3.4	-2.7
		(-1.1)	(-6.3)	(-11.1)	(-3.0)	(-2.6)
RNA polymerase II 15-kDa subunit	XM_643999	1.0	-1.2	1.1	-1.3	-1.3
		(1.4)	(1.2)	(1.2)	(1.1)	(1.2)

The common names, accession numbers, and fold changes of the selected genes upon L-cysteine deprivation are shown. The upper values are the fold changes in the expression obtained from qRT-PCR. The corresponding fold changes in the expression values obtained from Affymetrix analysis are shown in brackets.

by the availability of the reactive oxygen species, and agree with the proposed function of ISFs in anaerobes in combating oxidative stress by reducing O_2 and H_2O_2 to water [28]. In addition to oxidative stress, ISFs and ISF-related proteins were also induced upon the deprivation of sulfate or L-cysteine in bacteria [29].

Effect of L-Cysteine deprivation on membrane transport

Adaptive response to altered environmental conditions may include a significant alteration in the gene expression of the membrane transporters that are involved in the intake or efflux of various metabolites. A total of 4 genes with putative transport functions were significantly modulated in response to the removal of L-cysteine from the culture medium (Figure 5A). Two genes (EHI_173950 and EHI_186810) encoding major facilitator super-family (MFS) transporters showed maximum induction of 14.6 (EHI_173950) and 3.5 fold (EHI_186810) at 6 h upon L-cysteine deprivation. The third gene (EHI_190460) that encodes for an amino acid transporter was also induced by 3.9 fold at 48 h, whereas the fourth gene (EHI_152720) that encodes a small conductance mechanosensitive ion channel was down-regulated by 3.7 at 12 h upon L-cysteine deprivation (Additional files 2 and 3). The increments (~2 fold) in L-serine and L-threonine levels upon L-cysteine deprivation [12] may be attributed to either increased expression of amino acid transporter or MFS transporter, or reversal of L-cysteine-mediated inhibition of their transporters.

MFS is a large superfamily of membrane transporters present ubiquitously in bacteria, archaea, and eukarya [30]. They are involved in the symport, antiport, or uniport of various substrates including sugars, phosphorylated glycolytic intermediates, amino acids, polyols, drugs, neurotransmitters, and osmolites [30]. MFS transporters from yeast and bacteria are known to be involved in the transport of the metabolites of L-cysteine biosynthetic pathway including L-cysteine and O-acetylserine [31,32]. L-Cysteine deprivation resulted in drastic increments in various metabolites such as SMC, OAS, glycerol 3-phosphate and isopropanolamine, and sharp decrements in L-cysteine and L-cystine [12]. Thus, it may be possible that these MFS transporters are involved in either intake or efflux of the metabolites modulated upon L-cysteine deprivation. As the contribution of L-cysteine biosynthetic pathway to L-cysteine synthesis is negligible, both L-cysteine and L-cystine are completely deprived upon L-cysteine deprivation. Under this condition, *E. histolytica* trophozoites may induce expression of certain high affinity L-cysteine or L-cystine transporters. The genome of *E. histolytica* contains about 24 different genes for MFS transporters [6]. However, exact substrate specificities, and physiological roles of these MFS transporters in *E. histolytica* remain to be established.

Effect of L-cysteine deprivation on general metabolism

Recently, we demonstrated that in addition to the drastic metabolic changes in SAA metabolism, L-cysteine also regulates other metabolic pathways including phospholipid and energy metabolism [12]. However, like SAA metabolism, most of the genes involved in phospholipid or energy metabolism showed only minor changes in their expressions in response to L-cysteine deprivation. However, some transcriptional changes in the expression of genes involved in energy metabolism were noted. Genes encoding hexokinase, phosphoglycerate mutase, and malate dehydrogenase were slightly down regulated (Additional file 1). Down-regulation of these genes may partially contribute to the overall decrease in the metabolic flux across glycolysis as

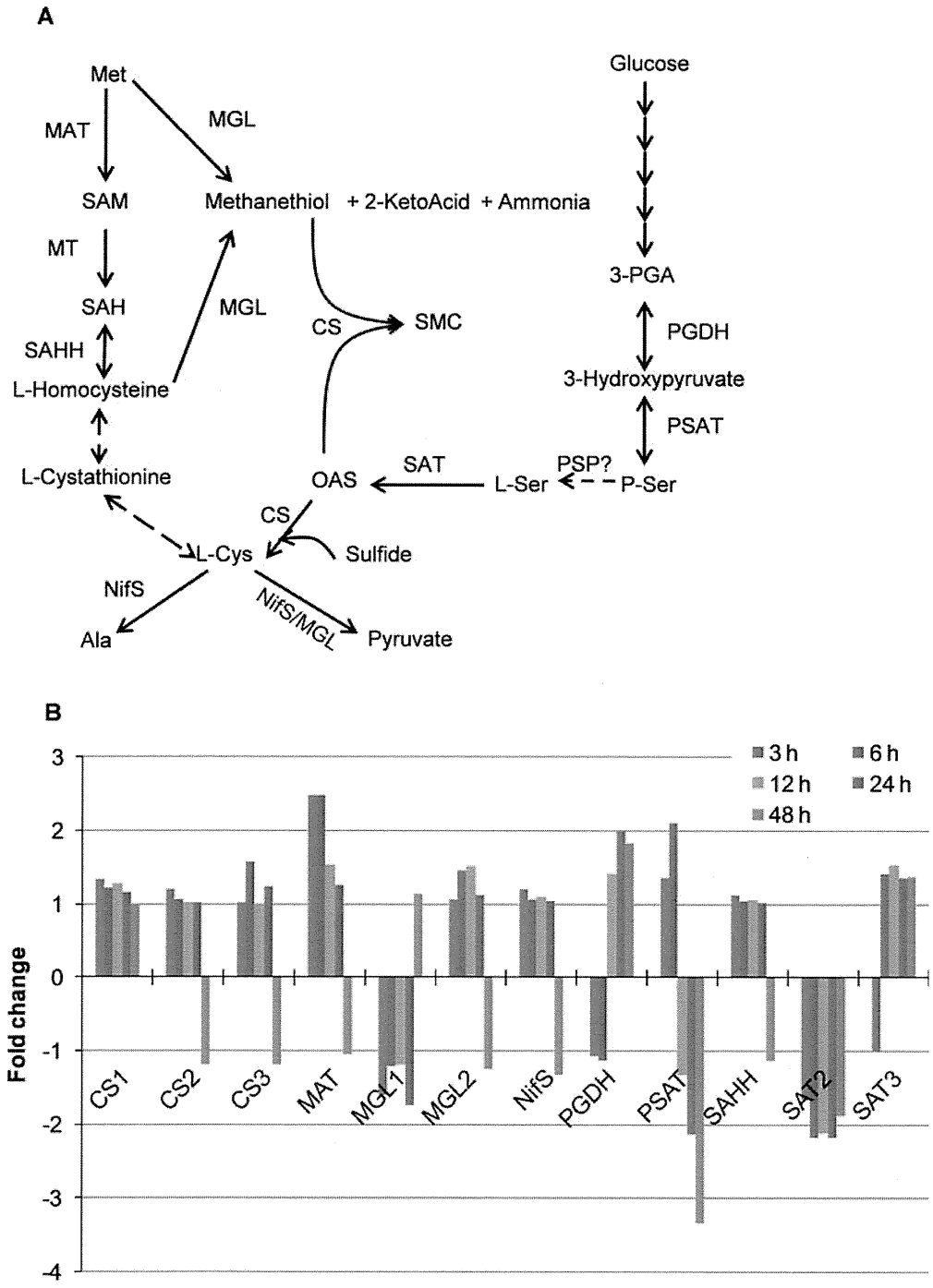

Figure 2 Effect of L-cysteine deprivation on expression of the genes involved in sulfur-containing amino acid metabolism. ***A***) General scheme of sulfur-containing amino acid metabolism in *E. histolytica*. Abbreviations: CS, cysteine synthase; SAT, serine O-acetyltransferase; PGDH, phosphoglycerate dehydrogenase; MGL, methionine γ-lyase; MAT, methionine adenosyl-transferase; MT, methyl-transferase; SAHH, S-adenosylhomocysteine hydrolase; NifS, cysteine desulfurase; PSAT, phosphoserine aminotransferase; PSP, phosphoserine phosphatase; OAS; O-acetylserine; SMC, S-methylcysteine; SAH, S-adenosylhomocysteine; SAM, S-adenosyltransferase; P-Ser, O-phosphoserine; 3-PGA, 3-phosphoglycerate. ***B***) Modulation of transcripts encoding enzymes involved in sulfur containing amino acid metabolism. Gene IDs: CS1, EHI_171750; CS2, EHI_160930; CS3, EHI_060340; MAT, 70.m00173; MGL1, EHI_144610; MGL2, EHI_142250; NifS; EHI_136380; PGDH, EHI_060860; PSAT, EHI_026360; SAHH, EHI_068250; SAT2, EHI_021570; SAT3, EHI_153430.

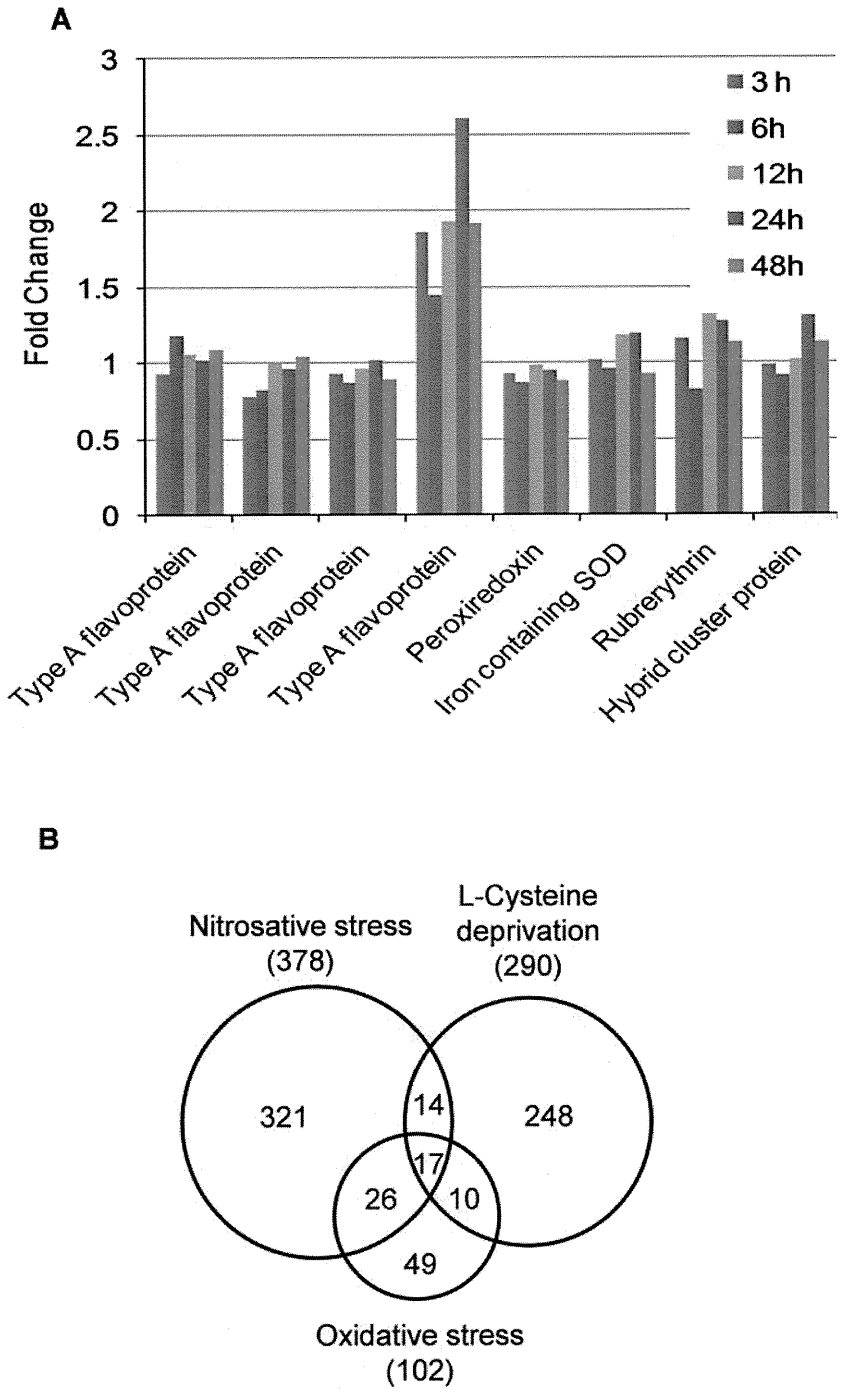

Figure 3 Comparison of the *E. histolytica* genes modulated upon L-cysteine deprivation and oxidative or nitrosative stress. ***A***) Expression kinetics upon L-cysteine deprivation of the genes previously inferred for oxidative and/or nitrosative stress defense. Gene/protein ID of enzymes are: type A flavoproteins (Flavodiiron proteins), EHI_159860, EHI_064530, EHI_096710, and EHI_129890; peroxiredoxin, EHI_145840; iron containing SOD, EHI_159160; rubrerythrin, EHI_134810; hybrid cluster protein, EHI_004600. **B***)* A Venn diagram showing the number of overlapping genes modulated upon L-cysteine deprivation and oxidative (1 mM of H_2O_2 for 1 h), or nitrosative stress (200 μM of DPTA-NONOate for 1 h), as described [23].

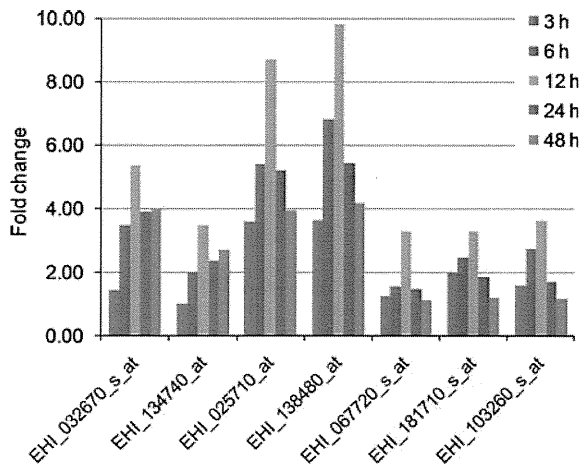

Figure 4 Induction of iron sulfur flavoproteins upon L-cysteine deprivation in *E. histolytica*. Values are expressed as fold changes of the transcripts under L-cysteine-deprived conditions, relative to the trophozoites cultured in medium containing normal concentration of L-cysteine.

reported in our previous metabolomic study of L-cysteine deprivation [12].

Transcripts that showed significant induction upon L-cysteine deprivation include a gene encoding putative glucosamine 6-phosphate N-acetyltransferase (EHI_080280), which is known to be involved in chitin biosynthetic pathway (Table 1). Two other genes encoding putative acetyltransferases (103.m00159, EHI_096770) were also induced 3-5 fold upon L-cysteine deprivation (Table 1; Additional file 2). These acetyltransferases contain maltose/galactose-O-acetyltransferase domains, and are known to be involved in the acetylation of a variety of substrates such as maltose, galactose, glucosamine, glucose, and fructose. However, the exact substrate specificity, physiological relevance, and the pathways that these acetyltransferases are involved in, are not known in *E. histolytica*. EHI_096770 was also induced upon H_2O_2-mediated oxidative (4 fold) or DPTA-NONOate-mediated nitrosative stress (2.7 fold) in *E. histolytica* [23]. A gene encoding cyst wall specific glycoprotein Jacob was induced during the early time points (Additional file 2). Both glucosamine 6-phosphate N-acetyltransferase and glycoprotein Jacob are involved in the encystation to form a chitin cell wall. However, it is not clear why the enzymes of chitin biosynthetic pathway are induced upon L-cysteine deprivation. Because some of the components of chitin biosynthetic pathway are known to be induced by oxidative stress [33], it is possible that stress induced by L-cysteine deprivation is also responsible for their induction.

A gene encoding riboflavin kinase/FAD synthetase that is involved in the synthesis of FAD or FMN cofactors was also induced up to 4.6 fold as an early response to L-cysteine deprivation (Table 1). This may imply that there is an increase demand of FMN or FAD cofactors during L-cysteine deprivation. A gene (EHI_086500) encoding short chain dehydrogenase/reductases (SDR) was also induced up to 8 fold during early time points. SDR are NAD^+/$NADP^+$-dependent oxido-reductases, and are similar to alcohol dehydrogenases (Table 1). Recently, we demonstrated that L-cysteine deprivation led to the accumulation of isopropanolamine, and *E. histolytica* possesses a pathway for its synthesis from methylglyoxal via aminoacetone [12]. SDR may be involved in the synthesis of isopropanolamine. Further biochemical analysis is required to better understand the significance of this L-cysteine-regulated dehydrogenase in *E. histolytica*.

In addition to the inductions of the genes discussed above, down-regulation of several genes encoding metabolic enzymes was also observed upon L-cysteine deprivation (Table 2; Additional file 3). L-Cysteine deprivation resulted in down-regulation of the expression of a gene encoding a novel NADPH-dependent oxido-reductase (EHI_045340). *E. histolytica* possesses two isotypes of these oxido-reductases (EhNO1 and 2) which contain FAD- and 2[4Fe-4S]-binding domains [34]. However, the expression of only EhNO2 (EHI_045340), but not of EhNO1, was dramatically down-regulated in a time-dependent manner upon deprivation of L-cysteine. This gene was also induced by 7 fold upon the supplementation of 10 mM of L-cysteine in to the culture medium for 48 h [34]. In contrast, the level of EhNO1 remained unchanged in either presence or absence of L-cysteine [34]. Our recent biochemical analysis showed that EhNO1 and 2 catalyse the NADPH-dependent reduction of oxygen to hydrogen peroxide, and L-cystine to L-cysteine, and also function as ferric and ferredoxin-$NADP^+$ reductases. EhNO2 possesses 4-fold higher L-cystine reduction efficiency than EhNO1, where as EhNO1 is more efficient in reducing ferredoxin and ferric ion [34].

L-Cysteine deprivation also led to the down regulation of two genes encoding dUTP nucleotidohydrolase, which convert dUTP to dUMP, and thus are involved in removing dUTP from the deoxynucleotide pool, reducing the probability of this nucleotide being mistakenly incorporated into DNA. Genes encoding aspartate aminotransferase and aspartate ammonia lyase which are involved in the catabolism of Glu, Asp, and Asn were down-regulated on L-cysteine deprivation (Additional file 3). These amino acids can be catabolised to pyruvate through malate and fumarate [35]. As a result of decreased utilization of pyruvate upon L-cysteine deprivation, malate and fumarate are accumulated. Down-regulation of aspartate aminotransferase, and aspartate